

Workshop on „Low Current, Low Energy Beam Diagnostics“
Hirschberg-Großsachsen, November 24-25, 2009

The SQUID based Cryogenic Current Comparator – an useful tool for beam diagnostics

Dr. sc. nat. Wolfgang Vodel
Friedrich-Schiller-Universität Jena
Low Temperature Laboratory

Outline



seit 1558

- Motivation
- Brief introduction to SQUID measurement technique
- **Cryogenic Current Comparator (CCC) principle**
- The CCC at GSI Darmstadt
- The CCC for DESY
- Experimental results
- Conclusions and Outlook

Motivation



seit 1558

In high energy physics there is a need for:

- Measurements of high energy ion beams in the range of $1 \mu\text{A} \dots 1 \text{nA}$ without back action (e.g. GSI Darmstadt)
- Measurements of so-called dark currents of superconducting acceleration cavities in the range below 50nA (e.g. DESY Hamburg)
- Measurements of charged particles in the CSR (e.g. MPI Heidelberg)

Solution: SQUID-based Cryogenic Current Comparator



seit 1558

Brief introduction to SQUID measurement technique

Superconducting **QU**antum **I**nterference **D**evice



seit 1558

SQUID is an acronym for **S**uperconducting **QU**antum **I**nterference **D**evice and is the most sensitive magnetic flux detector known today.

The working principle makes use of:

- **superconductivity**,
- the **flux quantization** in superconducting rings, and
- the **Josephson effect**.

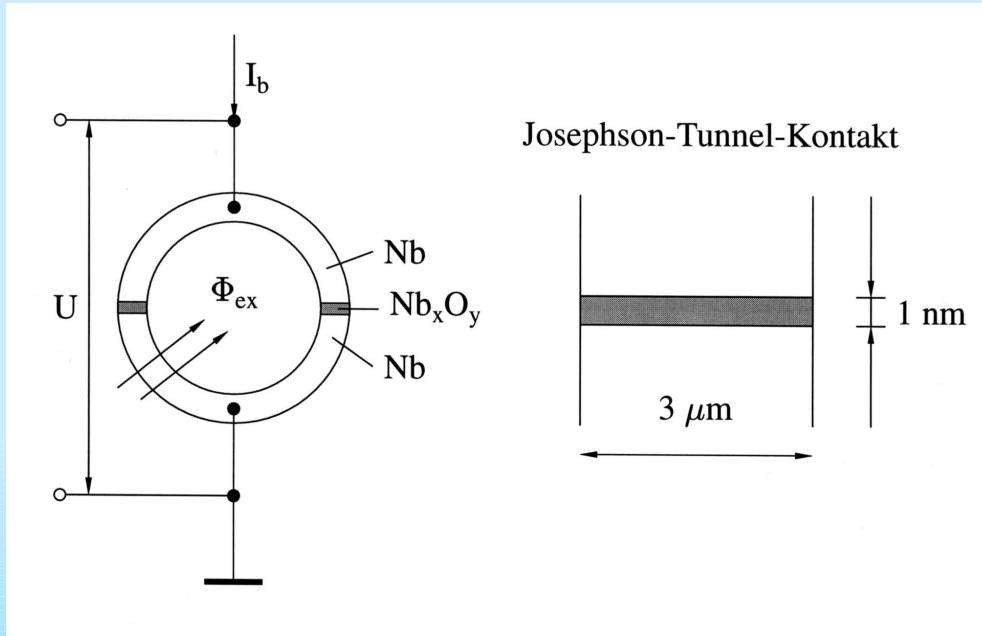
In principle, the SQUID consists of a superconducting ring with one or two weak links (Josephson tunnel junctions). We differ between:

- **dc SQUID** with two Josephson junctions and
- **rf SQUID** with one Josephson junction only.

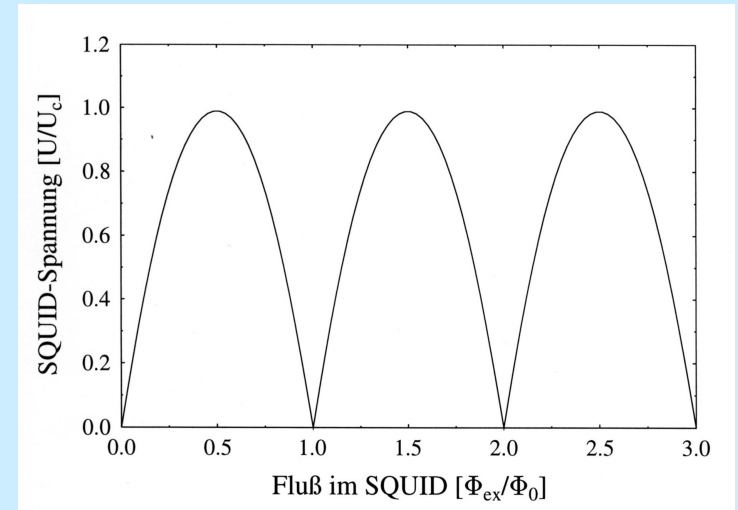
DC-SQUIDS



seit 1558



Simplified scheme of a dc-SQUID and a tunnel junction

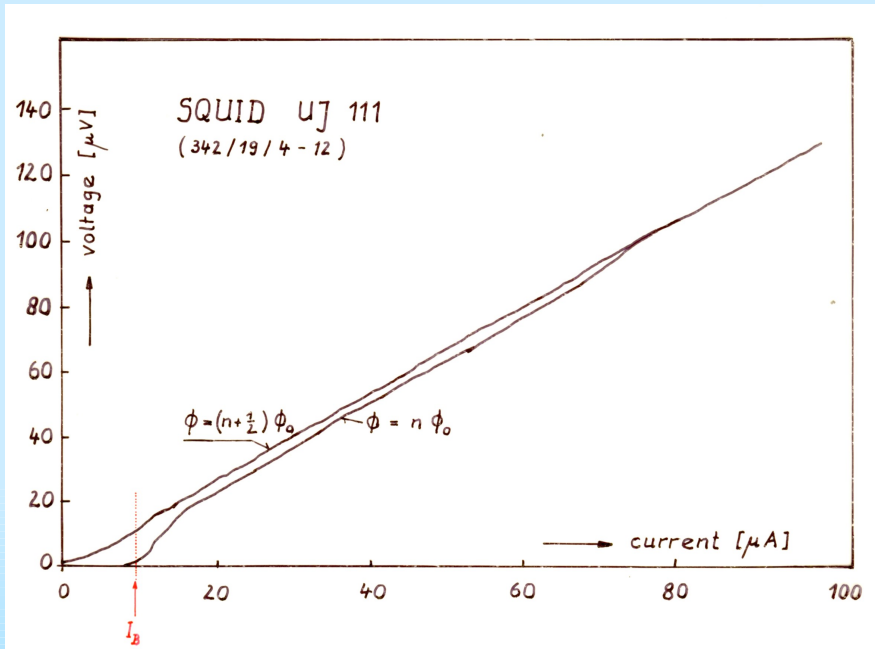


Output voltage of the SQUID vs. external magnetic flux

SQUID-Characteristics

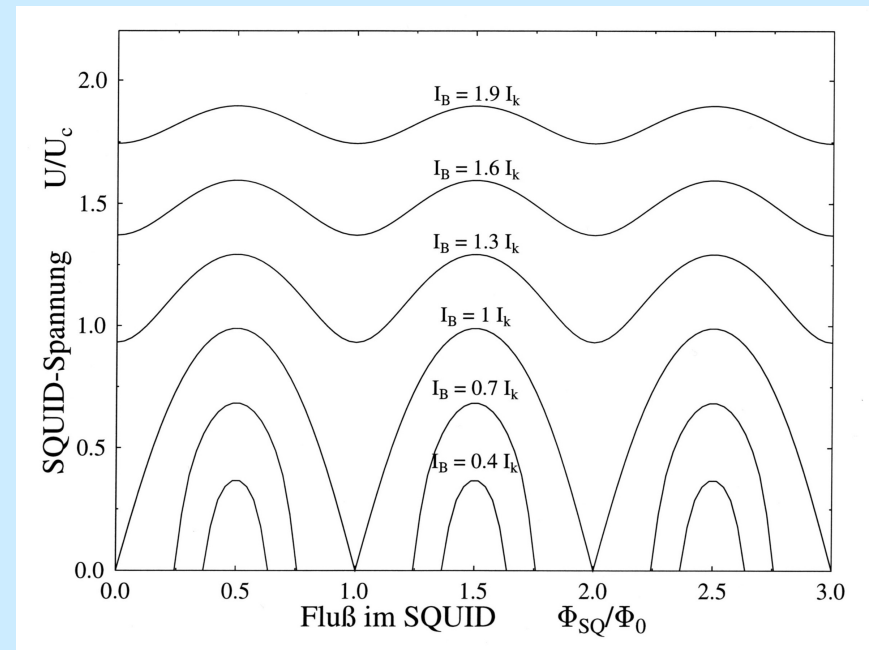


seit 1558



Voltage-Current-Characteristic of the SQUID UJ 111

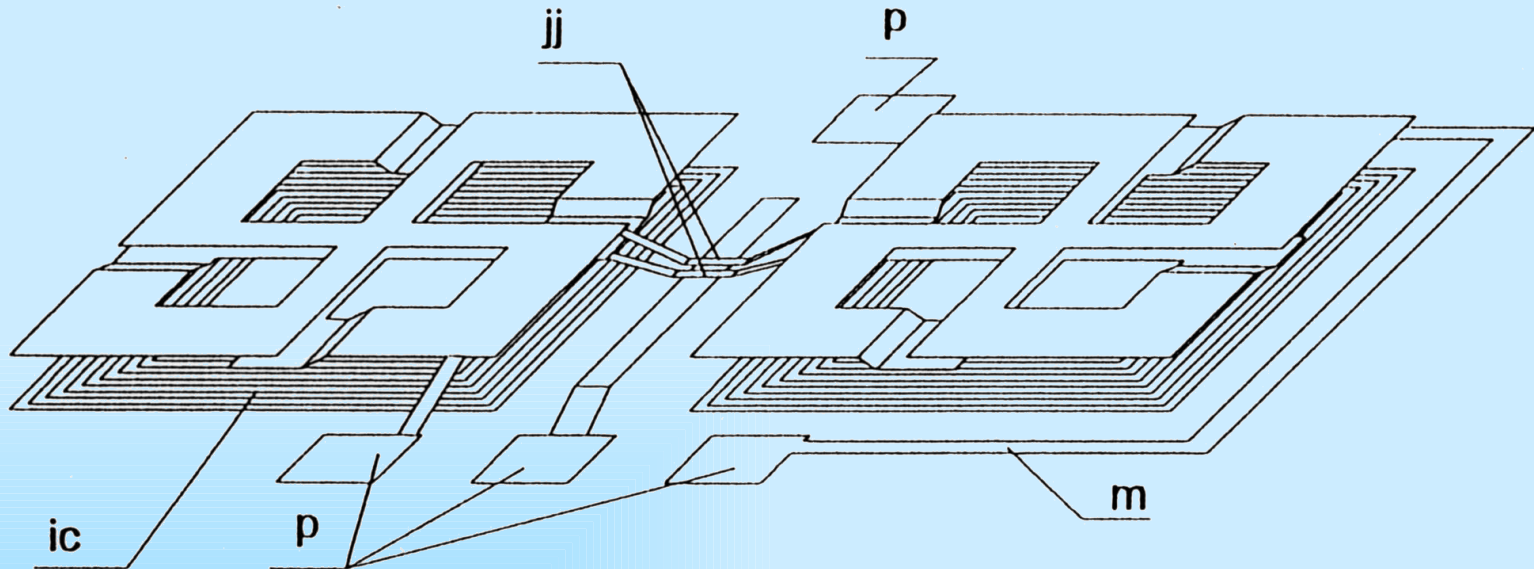
Output voltage of the SQUID vs. external flux for different bias currents



DC-SQUID lay-out



seit 1558



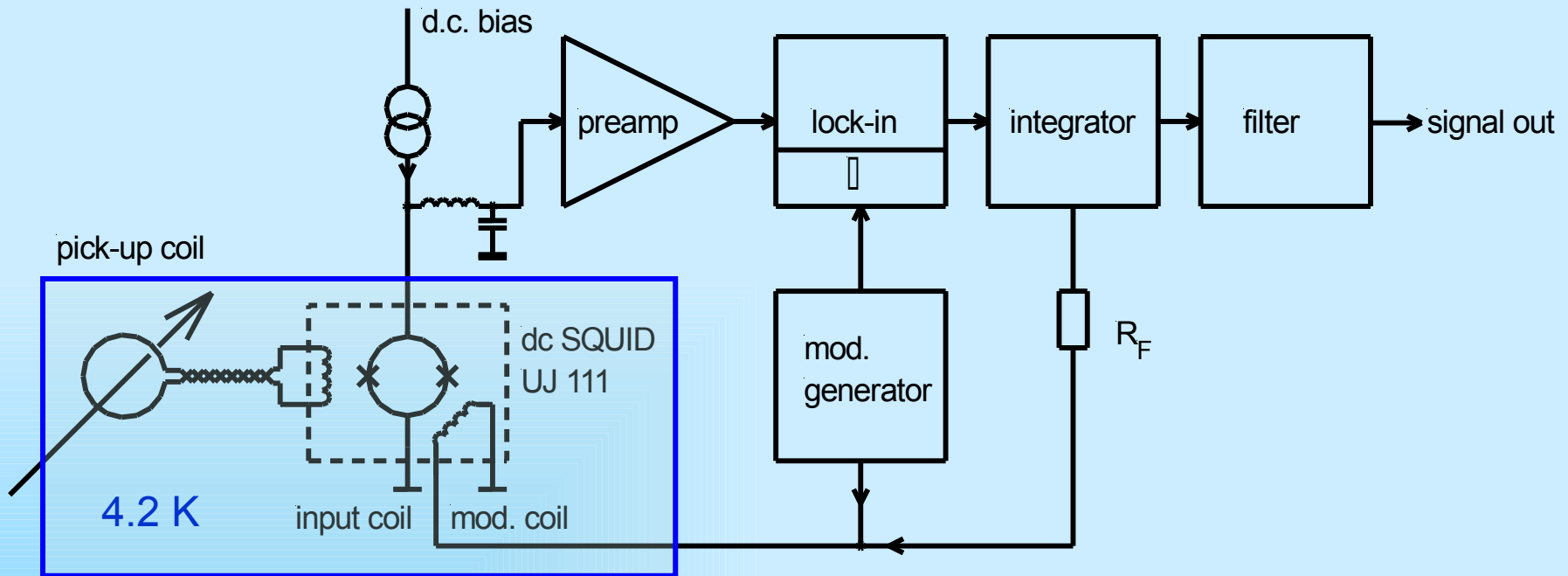
Simplified structure of the DC-SQUID *UJ 111* (FSU Jena).

jj: Josephson junctions, p: Nb contact pads, m: modulation coil,
ic: input coil

Block diagram of the *dc SQUID system 5*



seit 1558

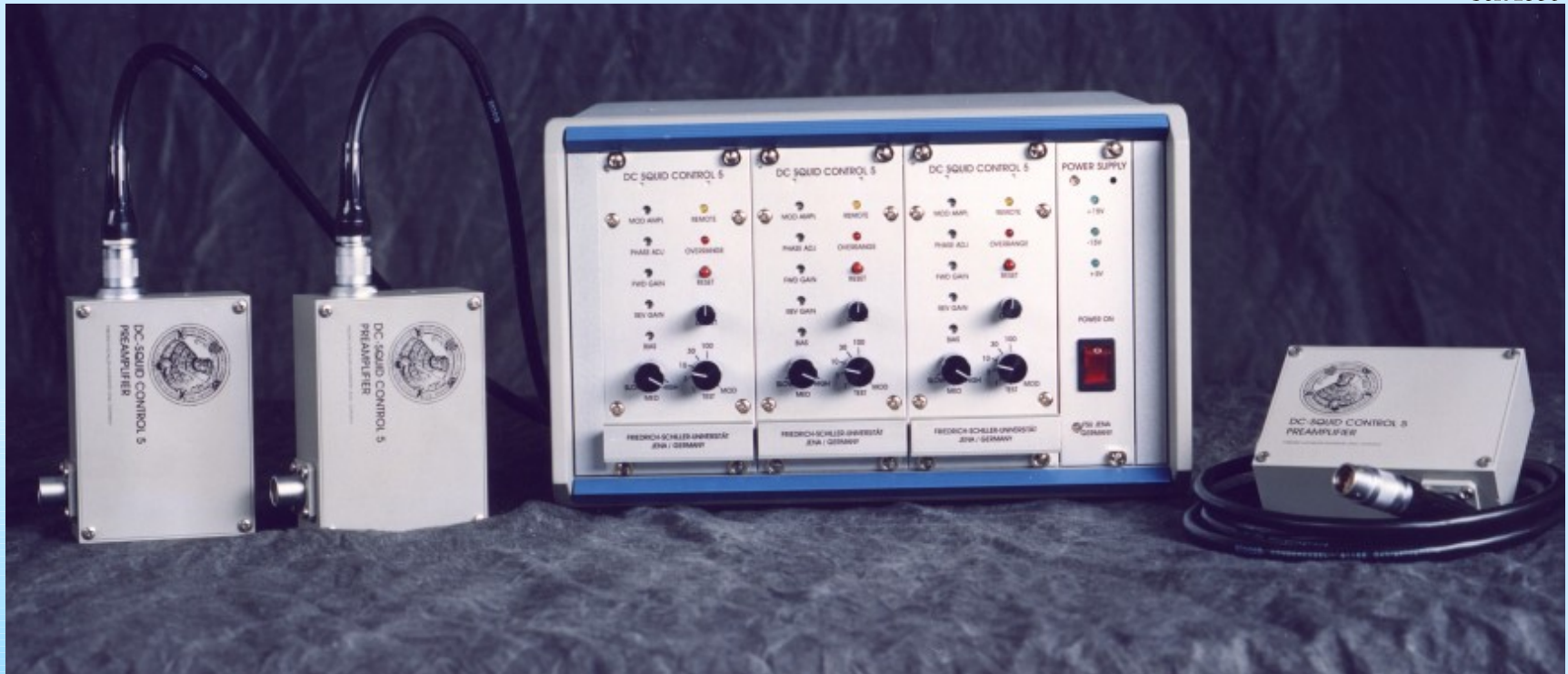


Simplified electrical scheme of the *dc SQUID electronics* of Jena University with the thin film *dc SQUID UJ 111*

The *dc SQUID system 5* of Jena University



seit 1558

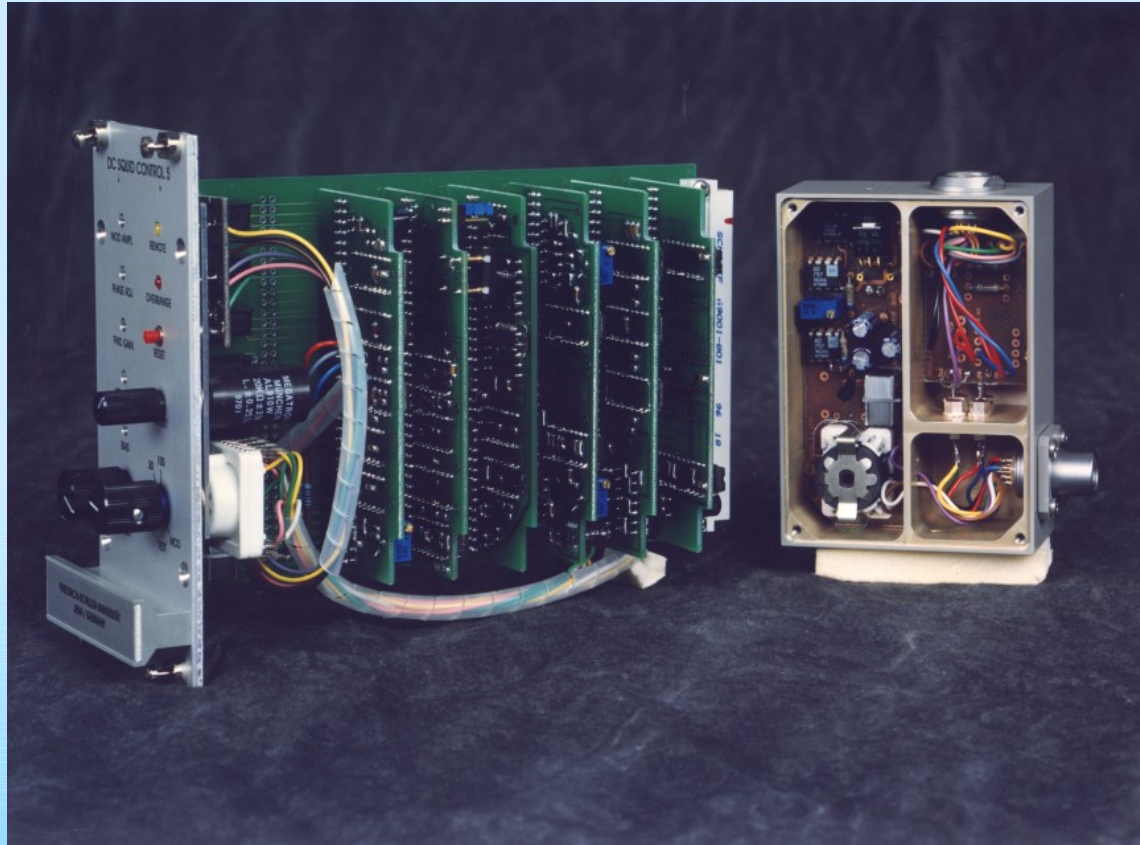


Photograph of the complete 3 channel *dc SQUID system 5* electronics with the connected low noise preamplifiers.

The *dc SQUID system 5* of Jena University



seit 1558



1 channel of the *dc SQUID system 5* (left) and the unclosed low noise preamplifier (right).



seit 1558

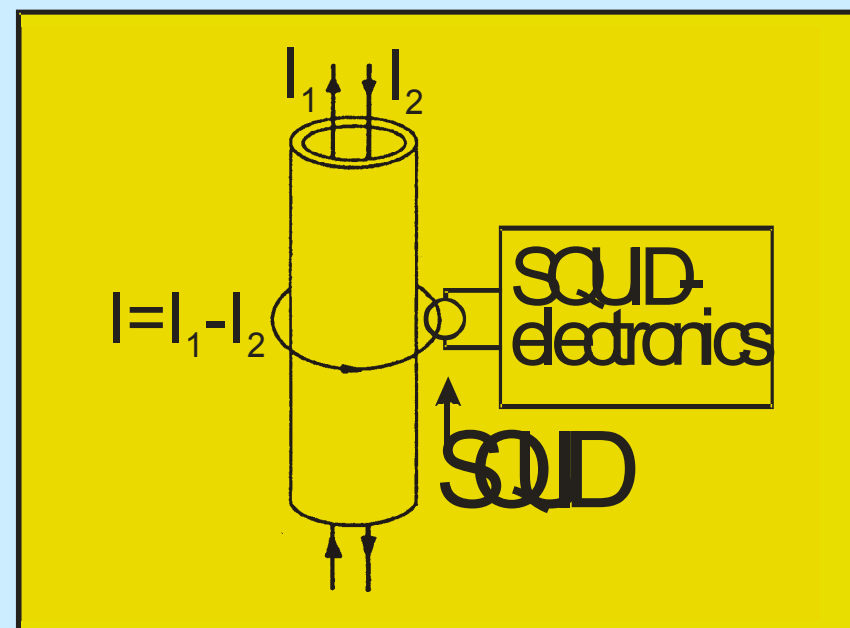
Main principle of the Cryogenic Current Comparator

The CCC, first developed in 1972 by Harvey[†], consists of:

- a superconducting pickup coil
- a high efficient superconducting shield
- a high performance SQUID measurement system

For absolute current measurements:

$$I = I_1 - I_2 = i_{\text{meas}} - 0$$



[†] Harvey, *Rev. Sci. Instrum.*, Vol. 43, p. 1626, 1972



seit 1558

Outstanding advantages of the CCC:

- Non destructive method
- High resolution ($< 1 \text{ nA}/\sqrt{\text{Hz}}$)
- Measurement of the absolute value of the current
- Exact absolute calibration using an additional wire loop
- Independency of charged particle trajectories
- Independency of charged particle energies

Resolution limits



seit 1558

The theoretical resolution of the CCC is limited, above all, by the thermal noise of the ferromagnetic core material:

- Thermal noise generates a noise current $\sqrt{\langle I^2 \rangle}$
- In connection with the inductance L this noise current gives rise of the magnetic flux noise $\Phi_{thermal}$
- For $SNR > 1$ the beam signal must meet the condition:

$$\Phi_{beam} = \int_A \vec{B} \cdot d\vec{f} \geq \Phi_{thermal} = L \cdot \sqrt{\langle I^2 \rangle}$$

Resolution limits



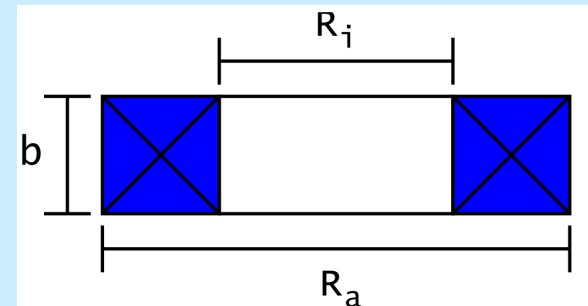
seit 1558

Minimum detectable current I_s :

$$I_s = \frac{2\pi \sqrt{k_B T L}}{\mu_0 \mu_r f(R_a, R_i, b)} \Rightarrow I_s \propto \frac{1}{\sqrt{\mu_r}}$$

where T denotes the temperature, μ_r the relative permeability of core material, n the number of windings (n=1), and L the inductance of pick-up coil according to:

$$L = n^2 \cdot \frac{\mu_0 \mu_r b}{2\pi} \ln \frac{R_a}{R_i}$$

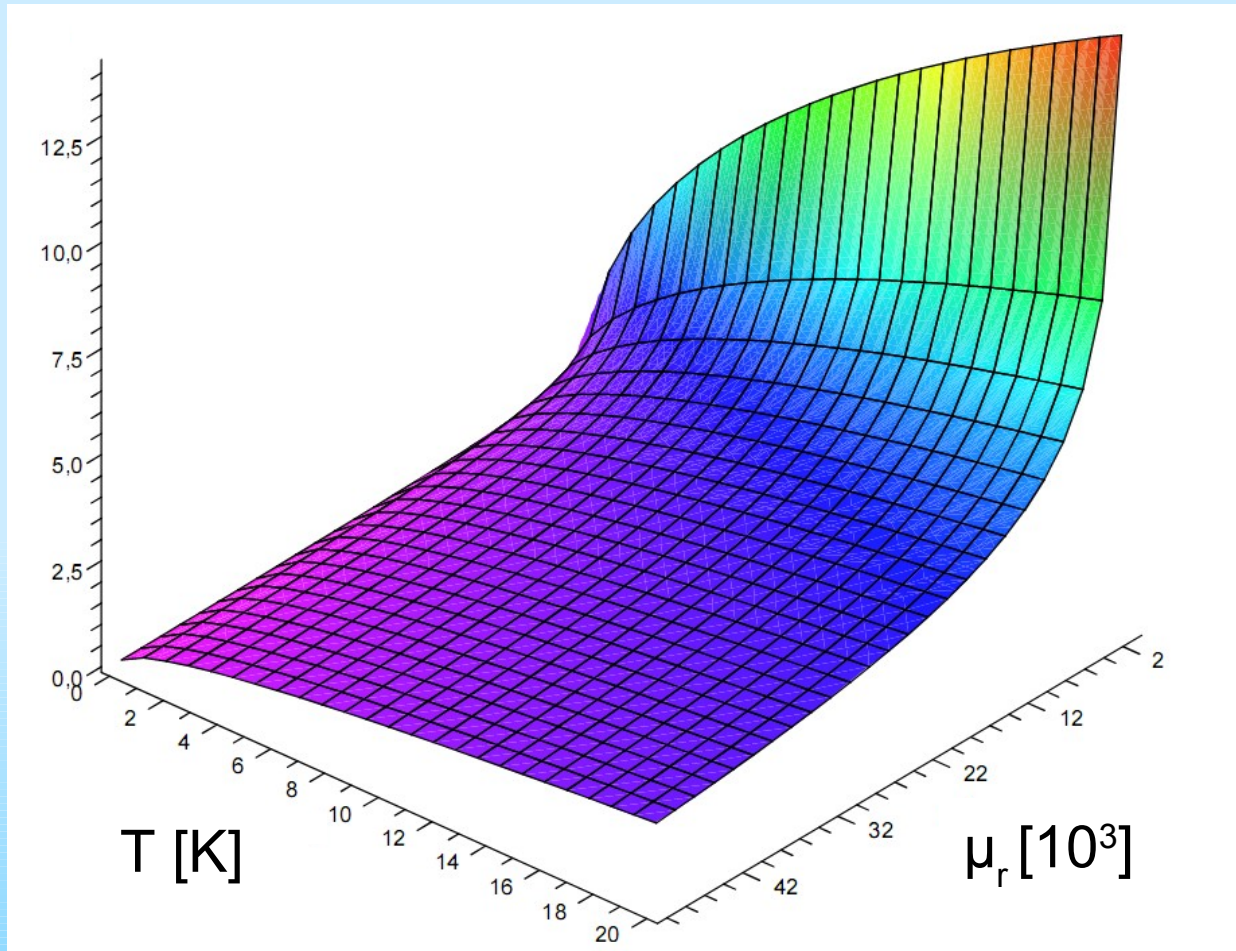


Resolution limits



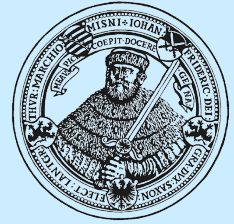
seit 1558

$I_s [10^{-9} \text{ A}]$



Minimum detectable current I_s as a function of temperature and relative permeability μ_r calculated for the currently used single turn toroidal pick-up coil.

Magnetic material



seit 1558

Vacuumschmelze Hanau

- **Vitrovac**

- tape material

- VC 6025, $\mu_r \sim 5.000$,

- VC 6155, $\mu_r \sim 2.000$

- toroidal tape wound cores

- VC 6025 F, VC 6030 F,

- VC 6150 F, VC 6200 F

- with different μ_r from 1.200
to 200.000 at 300 K

- **Vitroperm**

- toroidal tape wound cores

- VP 250 F, VP 500 F

- with different μ_r from 6.000
to 130.000 at 300 K

Magnetec Langenselbold

- **Nanoperm**

- toroidal tape wound cores in plastic
cases in different dimensions
with μ_r from 25.000 to 100.000 at
300 K

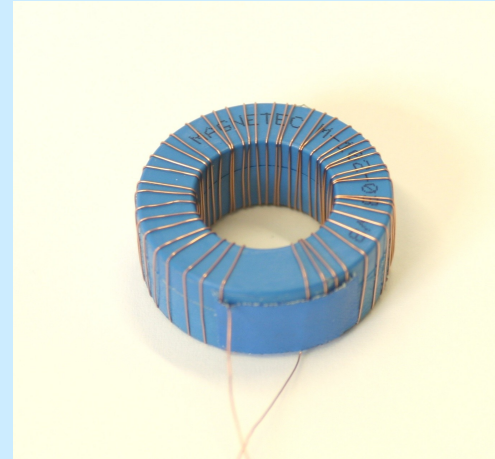
Nanoperm- magnetic cores



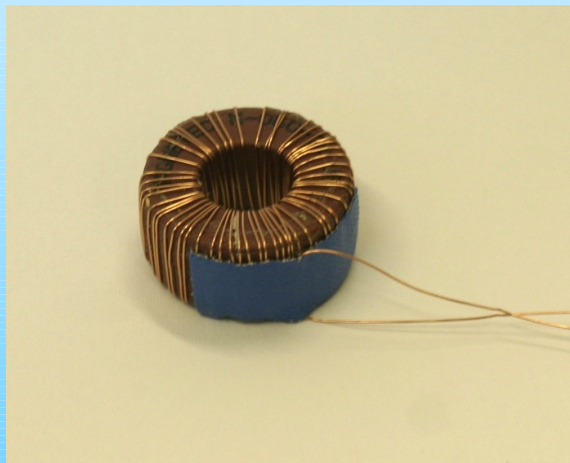
seit 1558



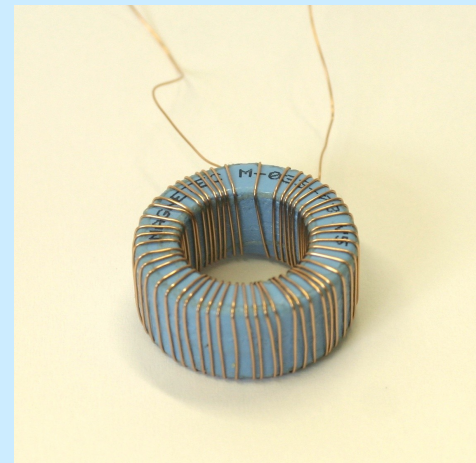
Nanoperm-toroidal tape wound cores



Nanoperm-toroidal tape wound cores
M074 (50 windings)



Nanoperm-toroidal tape wound cores M060
(50 windings)

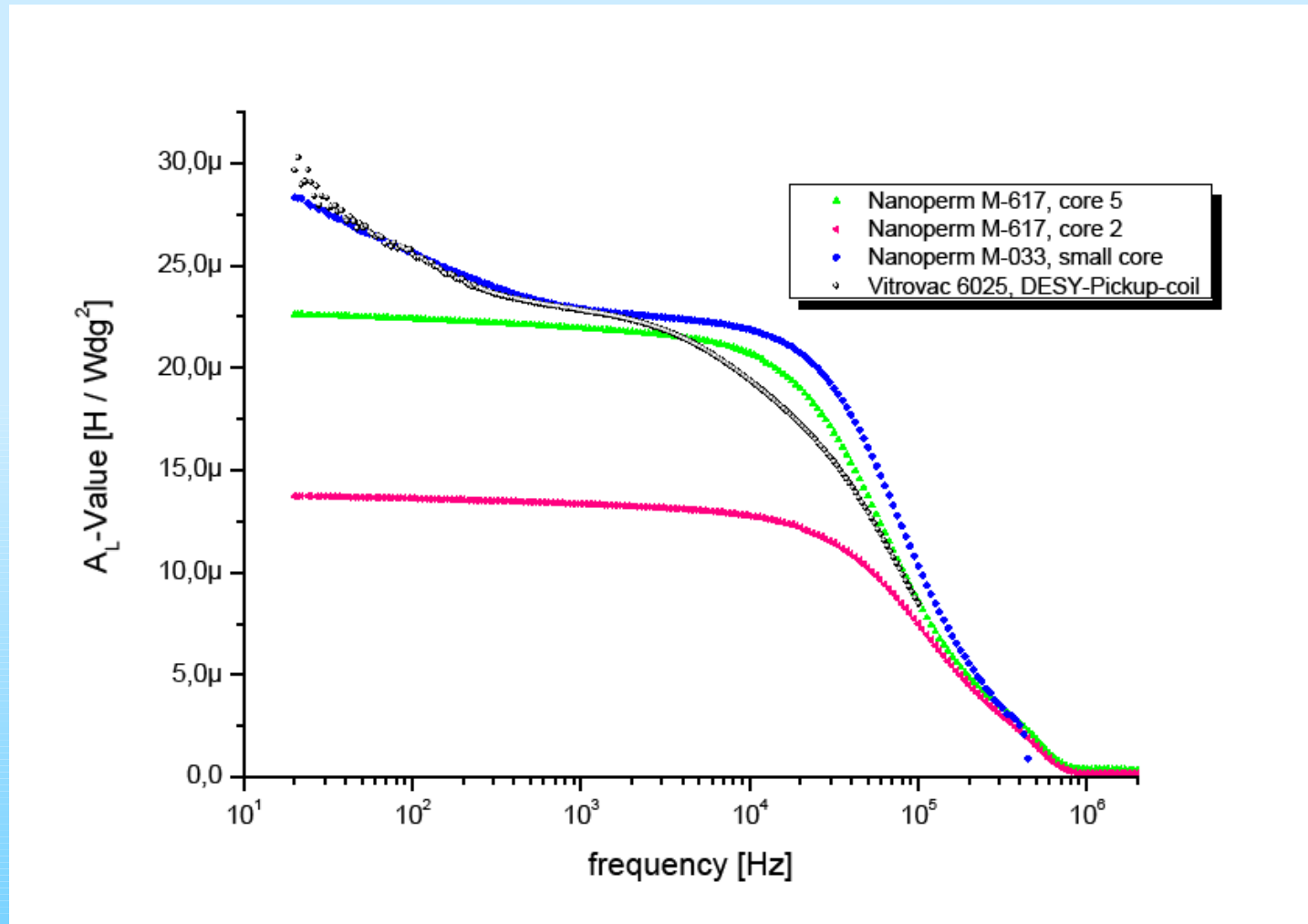


Nanoperm-toroidal tape wound cores
M033 (50 windings)

A_L -values of magnetic materials at low temperatures



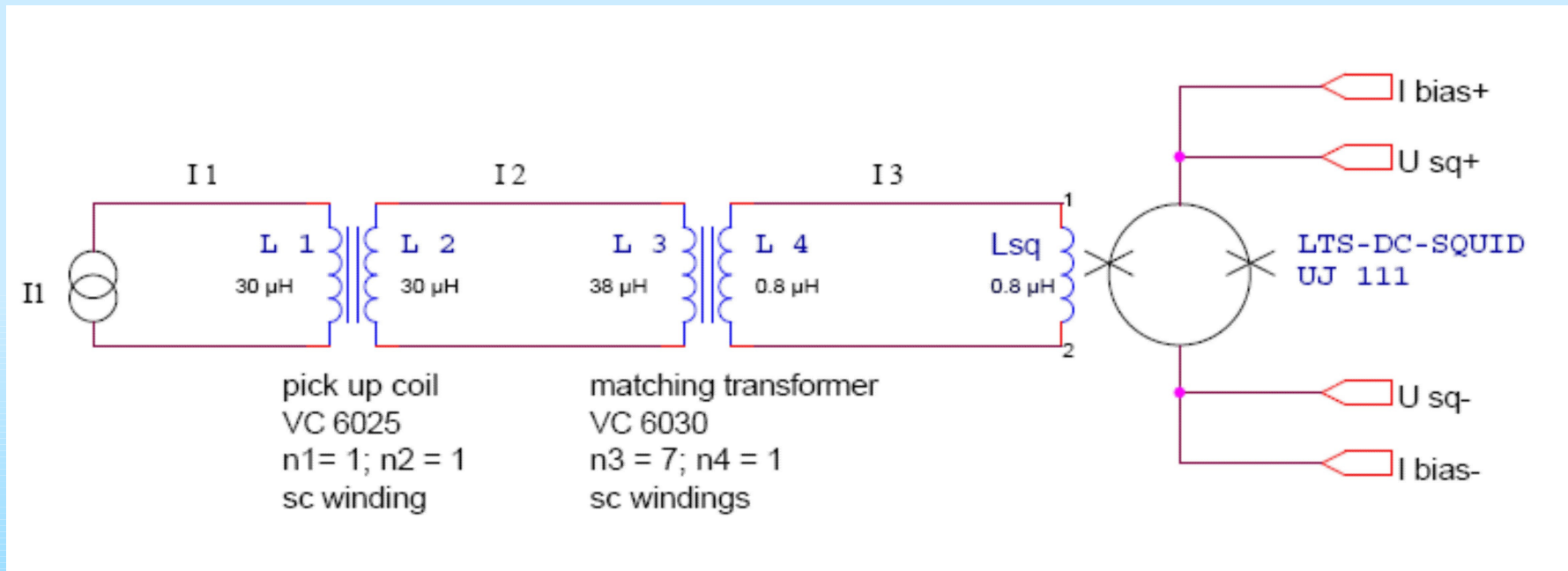
seit 1558



Electrical Scheme of the input circuit



seit 1558



Current gain



seit 1558

Short circuit current gain
of a transformer:

$$\frac{I_2}{I_1} = \frac{n_1}{n_2}$$

Current gain of a
stressed transformer
with an inductive load:

$$\frac{I_2}{I_1} = \frac{n_1}{n_2} \cdot \frac{1}{1 + \frac{L_l}{L_2}}$$

Total current gain of the
system

(pick up coil – matching
transformer – SQUID
input coil:

$$\frac{I_3}{I_1} = \frac{n_3}{n_4} \cdot \frac{1}{1 + \frac{L_{SQ}}{L_4}} \cdot \frac{n_1}{n_2} \cdot \frac{1}{1 + \frac{L_3 \cdot L_{SQ}}{(L_4 + L_{SQ}) \cdot L_2}}$$

Applications of the CCC



seit 1558

- Measurement of high energy ion currents of accelerators

Current resolution: $\leq 250 \text{ pA}/\sqrt{\text{Hz}}$

(GSI Darmstadt)

- Measurement of so-called dark currents of RF accelerator cavities

Current resolution: $\leq 40 \text{ pA}/\sqrt{\text{Hz}}$

(DESY Hamburg)

Supercond. Sci. Technol. 20, pp. 393-397 (2007)



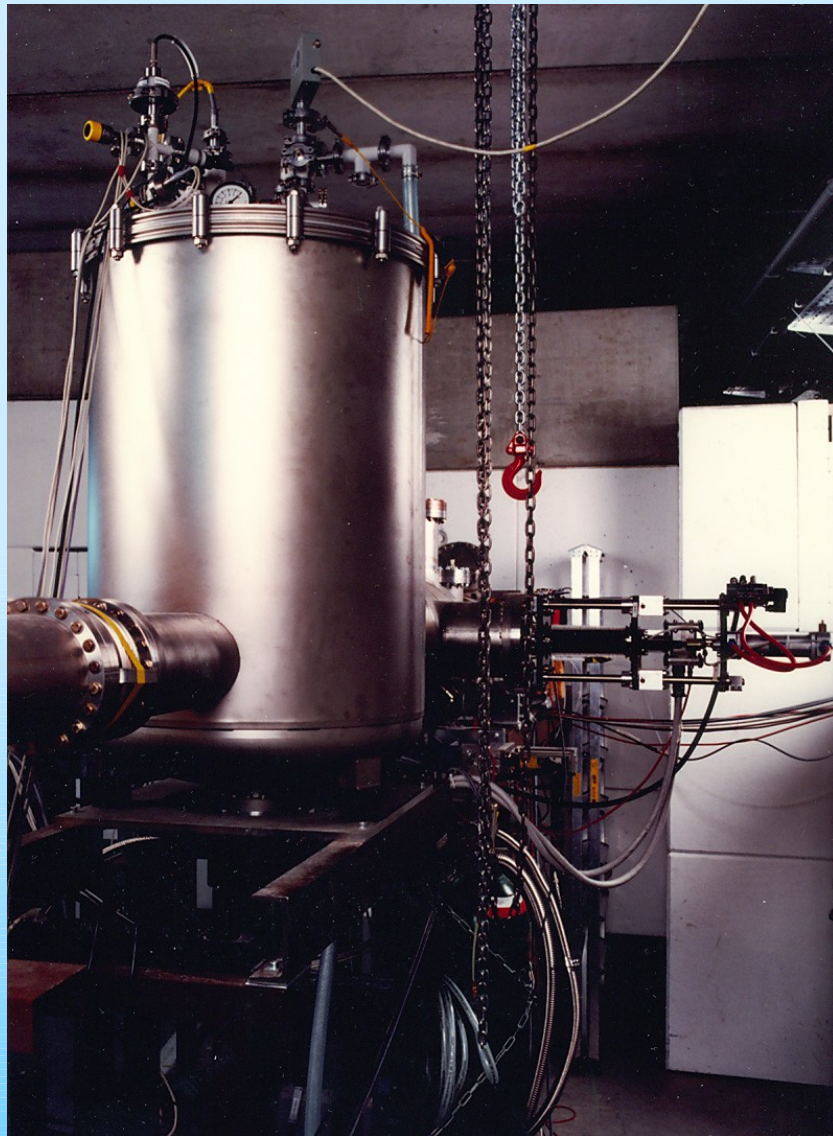
seit 1558

The CCC at GSI Darmstadt

The CCC at GSI Darmstadt



seit 1558



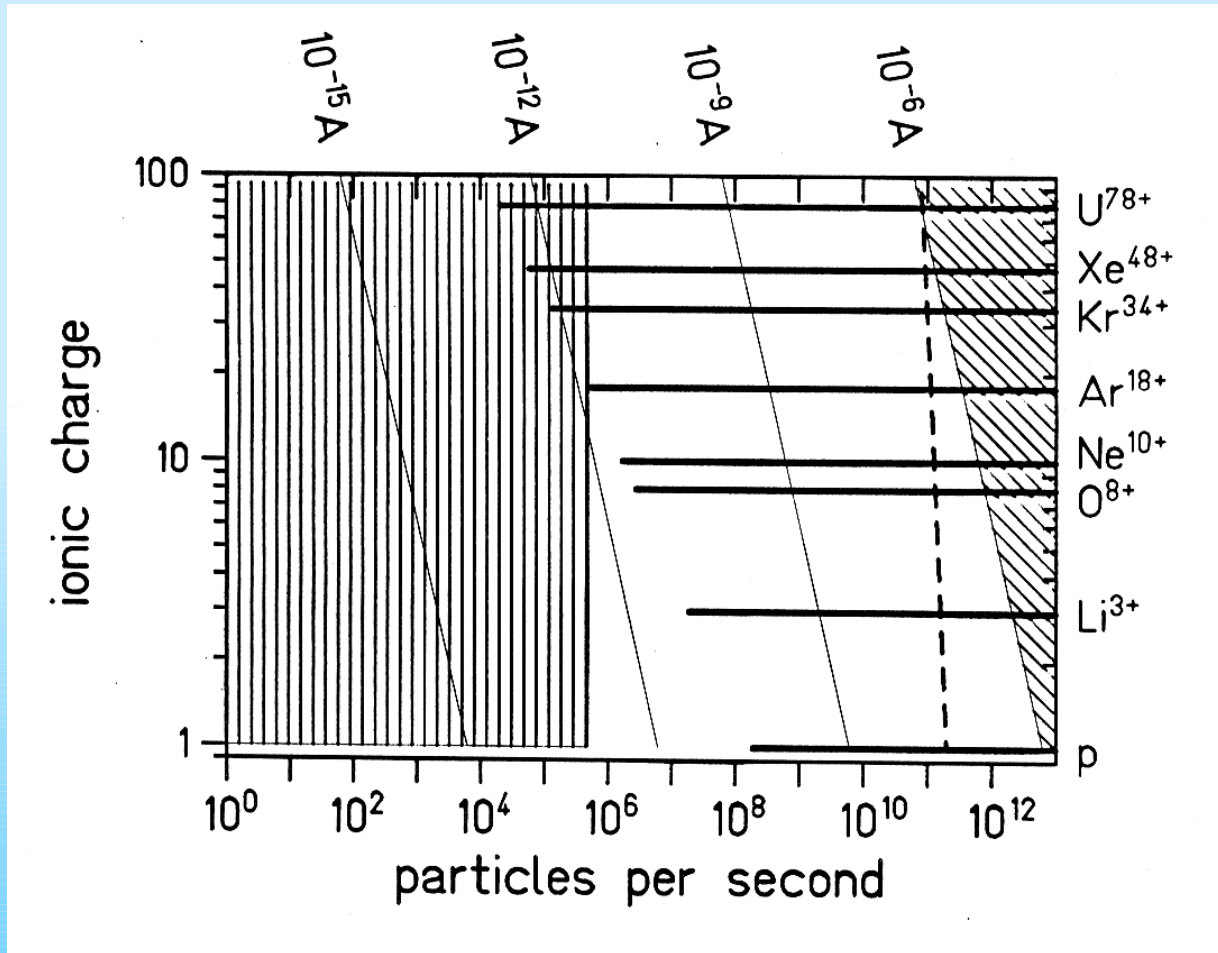
GSI (Darmstadt) and the Friedrich Schiller University Jena made an impressive demonstration of the capabilities of a CCC to measure extracted high energy ion-beams (Ar, Ne) with a resolution of:

0.25 nA/ $\sqrt{\text{Hz}}$.

Motivation for the CCC at GSI Darmstadt



seit 1558



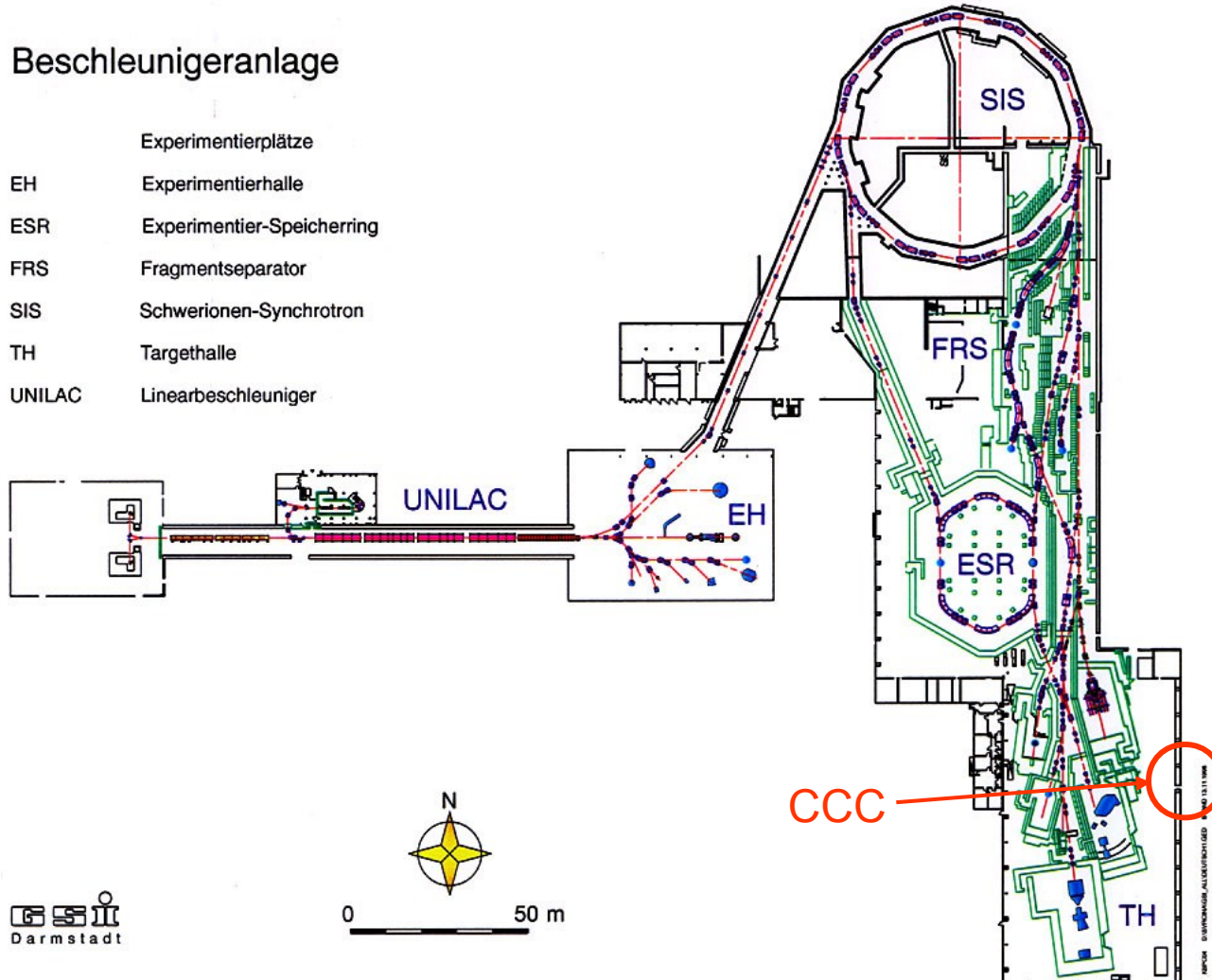
The SIS at GSI Darmstadt



seit 1558

Beschleunigeranlage

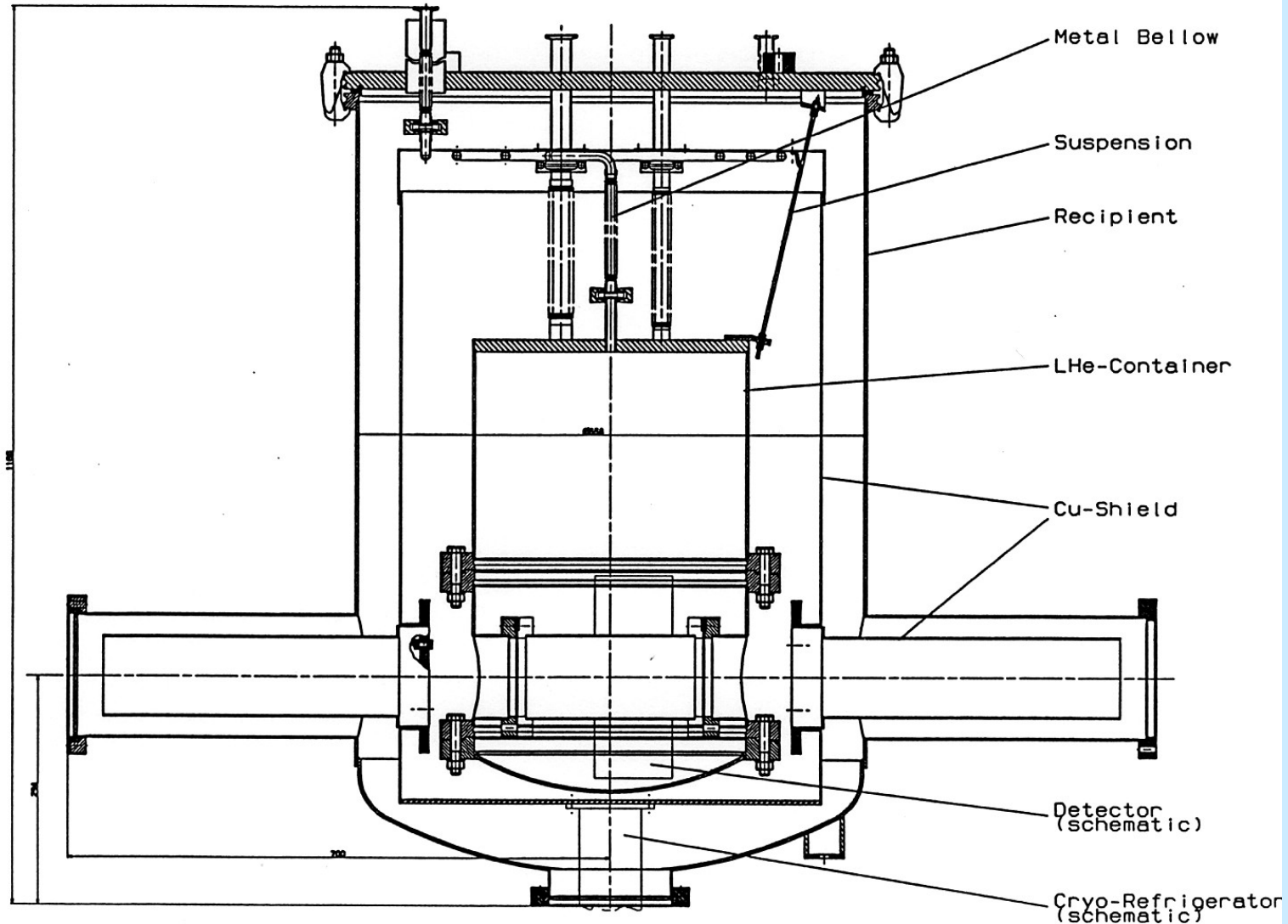
	Experimentierplätze
EH	Experimentierhalle
ESR	Experimentier-Speicherring
FRS	Fragmentseparator
SIS	Schwerionen-Synchrotron
TH	Targethalle
UNILAC	Linearbeschleuniger



Cross section of the CCC



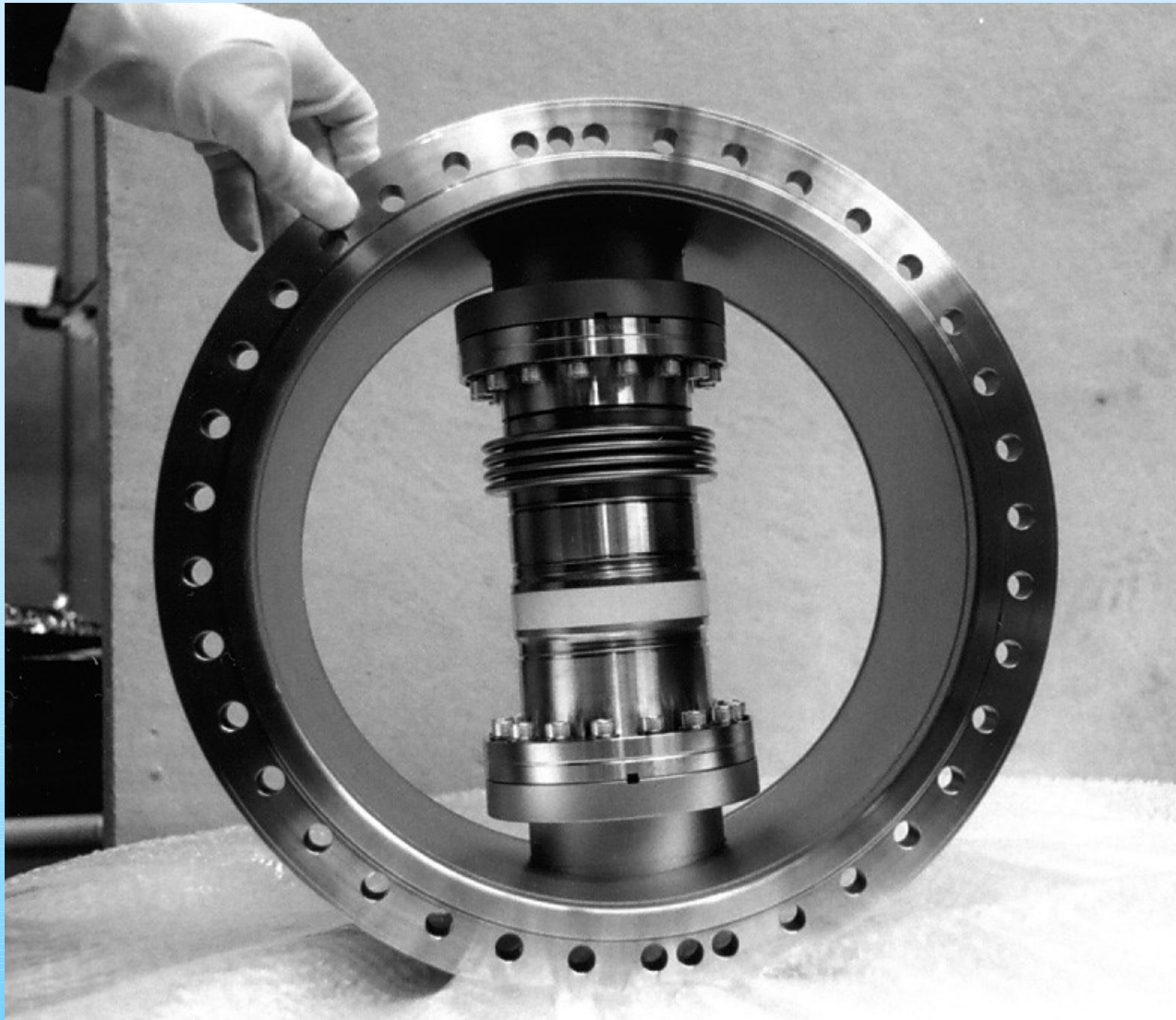
seit 1558



Technical details of the CCC



seit 1558



First beam measurement ($^{20}\text{Ne}^{10+}$)

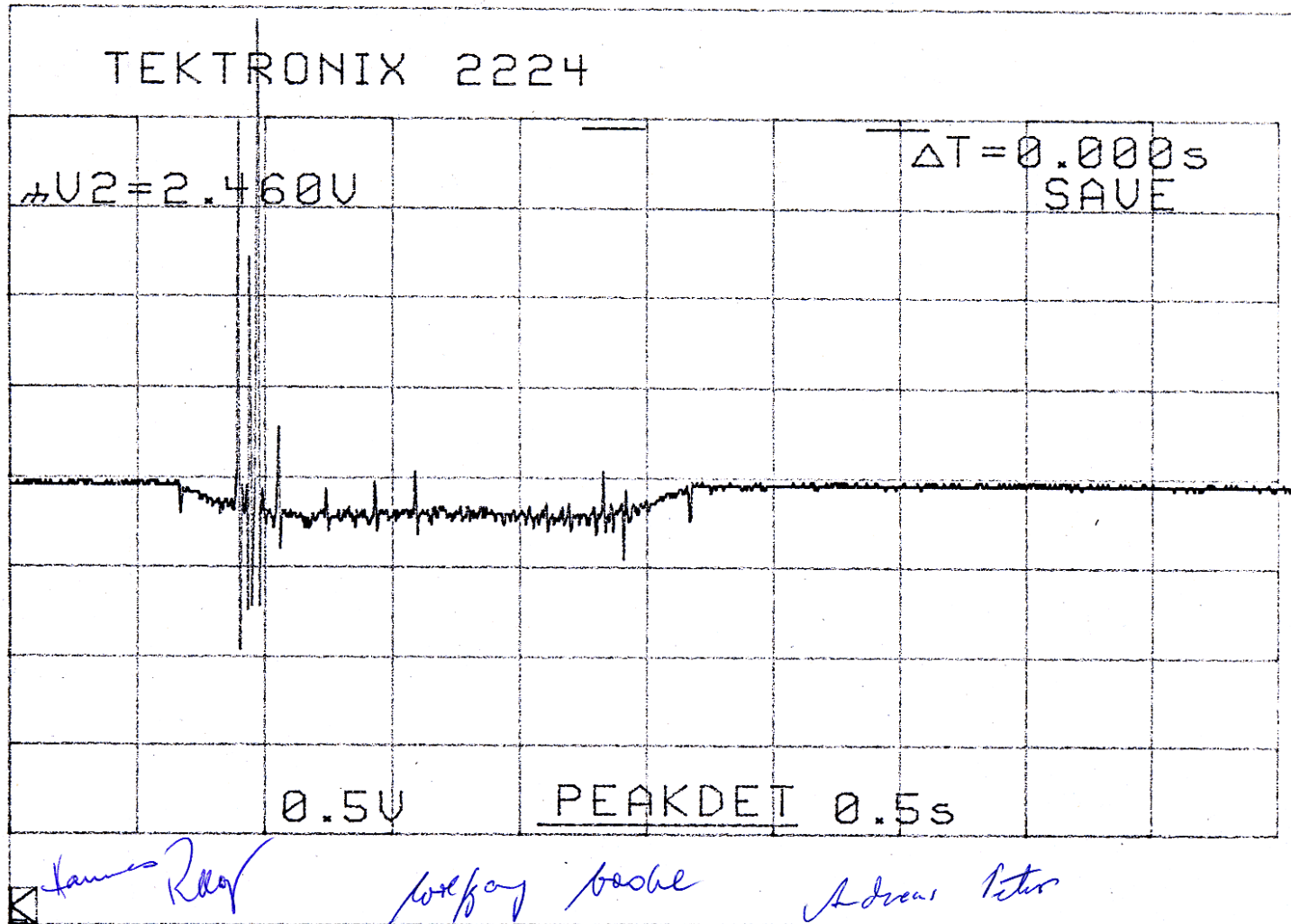


seit 1558

8.5.1996

146-40

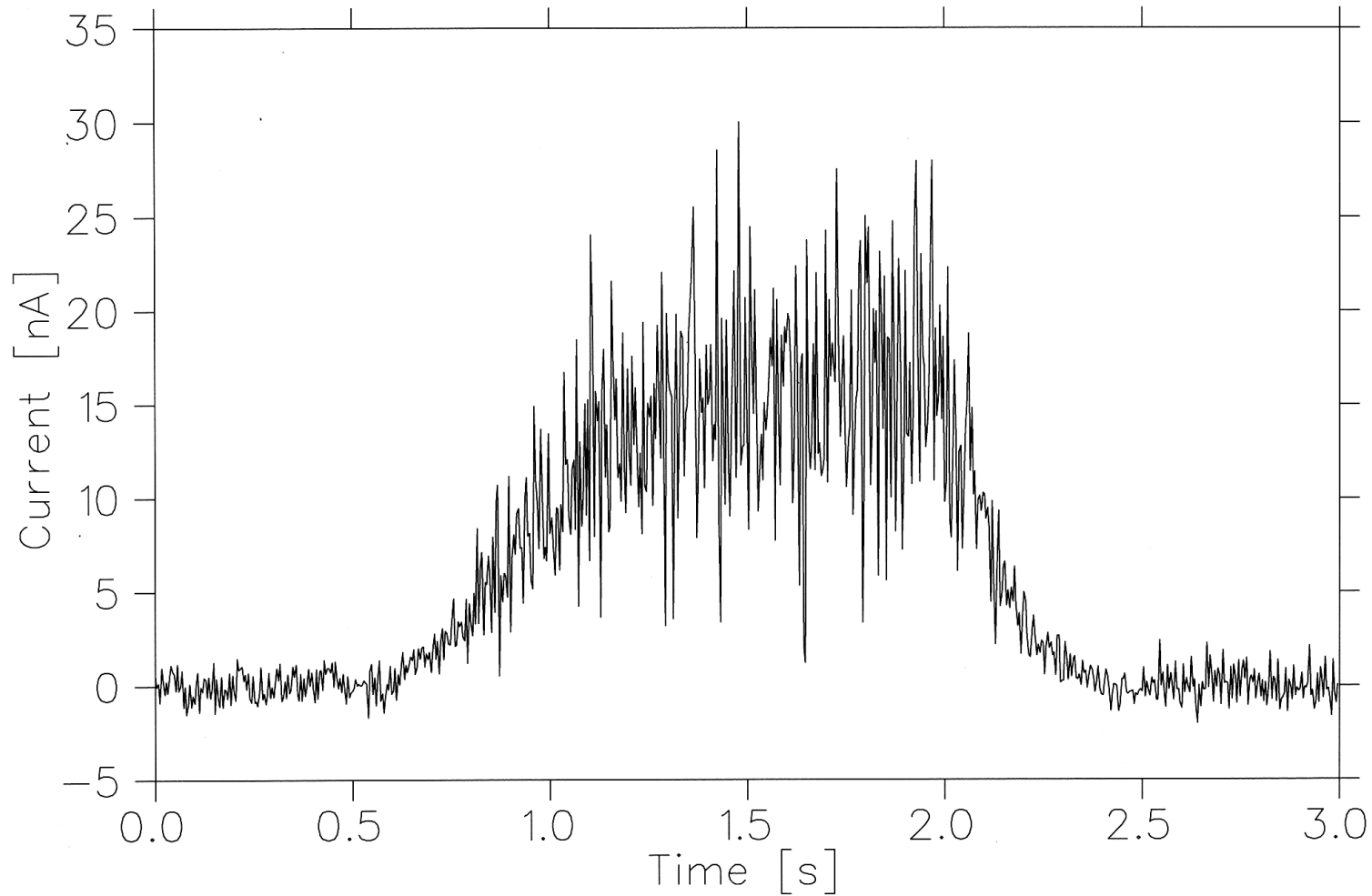
Sens.: x 1, 100 kHz



High resolution beam measurement



seit 1558





seit 1558

The CCC at DESY Hamburg

Motivation



seit 1558

The performance of superconducting cavities of accelerators is characterized by the Q-value vs. gradient dependency, measured in a cavity test stand (e. g. “*CHECHIA*” at DESY or “*HoBiCaT*” at BESSY).

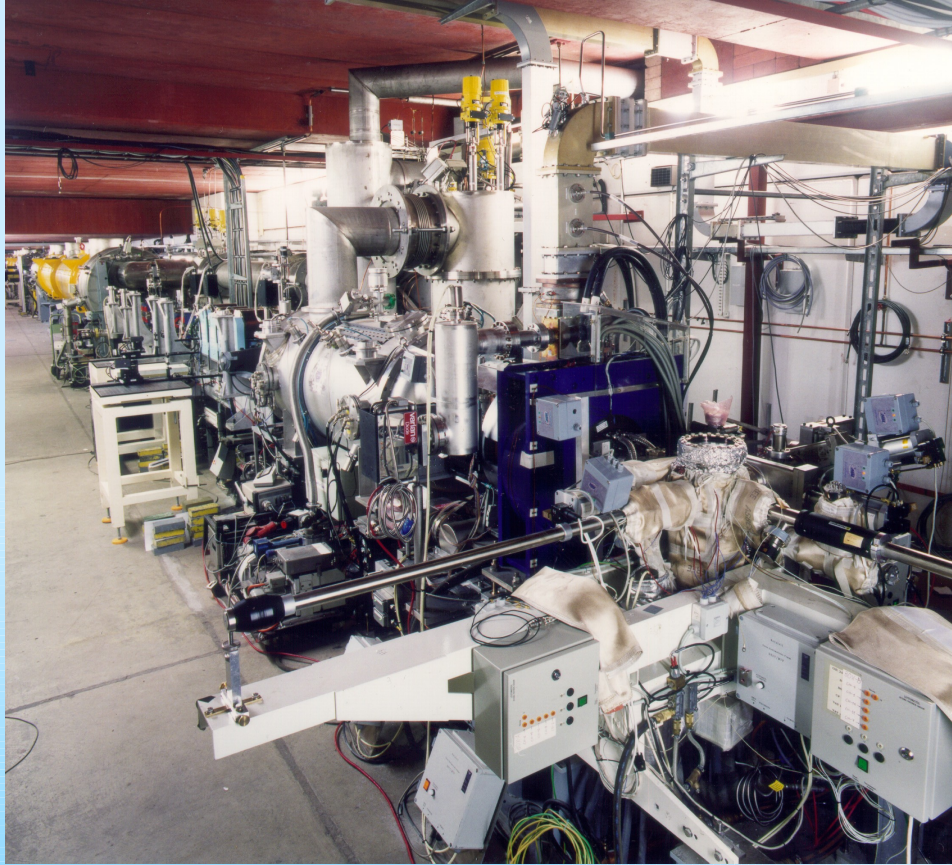
But unfortunately there is:

“The existence of so-called ***dark currents*** (vs. gradient) which may have an influence on the accelerator operation”.

The CCC for X-FEL



seit 1558



In collaboration with Jena University, GSI and DESY a CCC for the measurement of dark currents of the X-FEL accelerator cavities is under construction.

Dark currents:



seit 1558

- Unwanted particle source
- Limit the accelerator performance by
 - Additional thermal load ($T = 1.8 \text{ K}$)
 - Propagating dark current
- An avalanche instability due to the propagating dark current arise if (statistically):
number of emitted electrons/cavity period > 1
- This limits the dark current of a 9-cell cavity to
 $i_{\text{dark}} < 50 \text{ nA}$

Dark currents:



seit 1558

- Are caused by field emission of electrons in high gradient fields
- The forces of the applied external field are higher than the bounding forces inside the crystal structure.

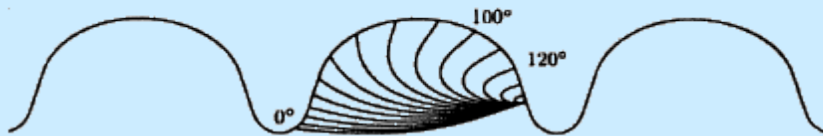
Potential emitters are:

- Imperfections of the cavity shape, e. g. corners, spikes and other discontinuities where occur high field gradients
- Imperfections of the crystal matter, e. g. grain boundaries
- Inclusion of “foreign” contaminants (In, Fe, Cr, Si, Cu,... microparticles)

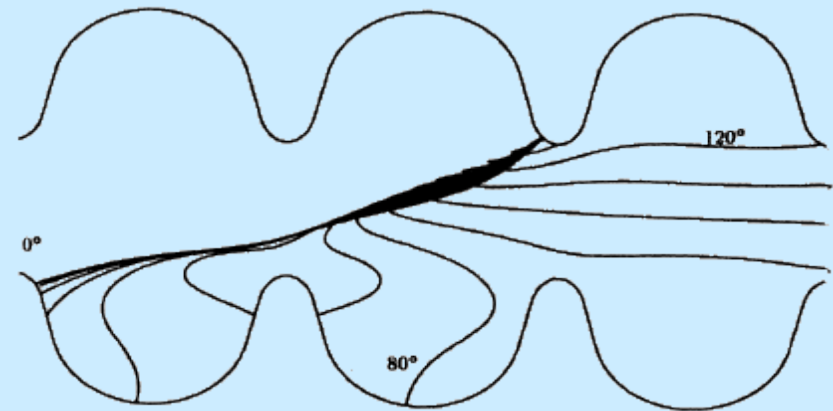
Dark current simulations



seit 1558



Dark current simulations



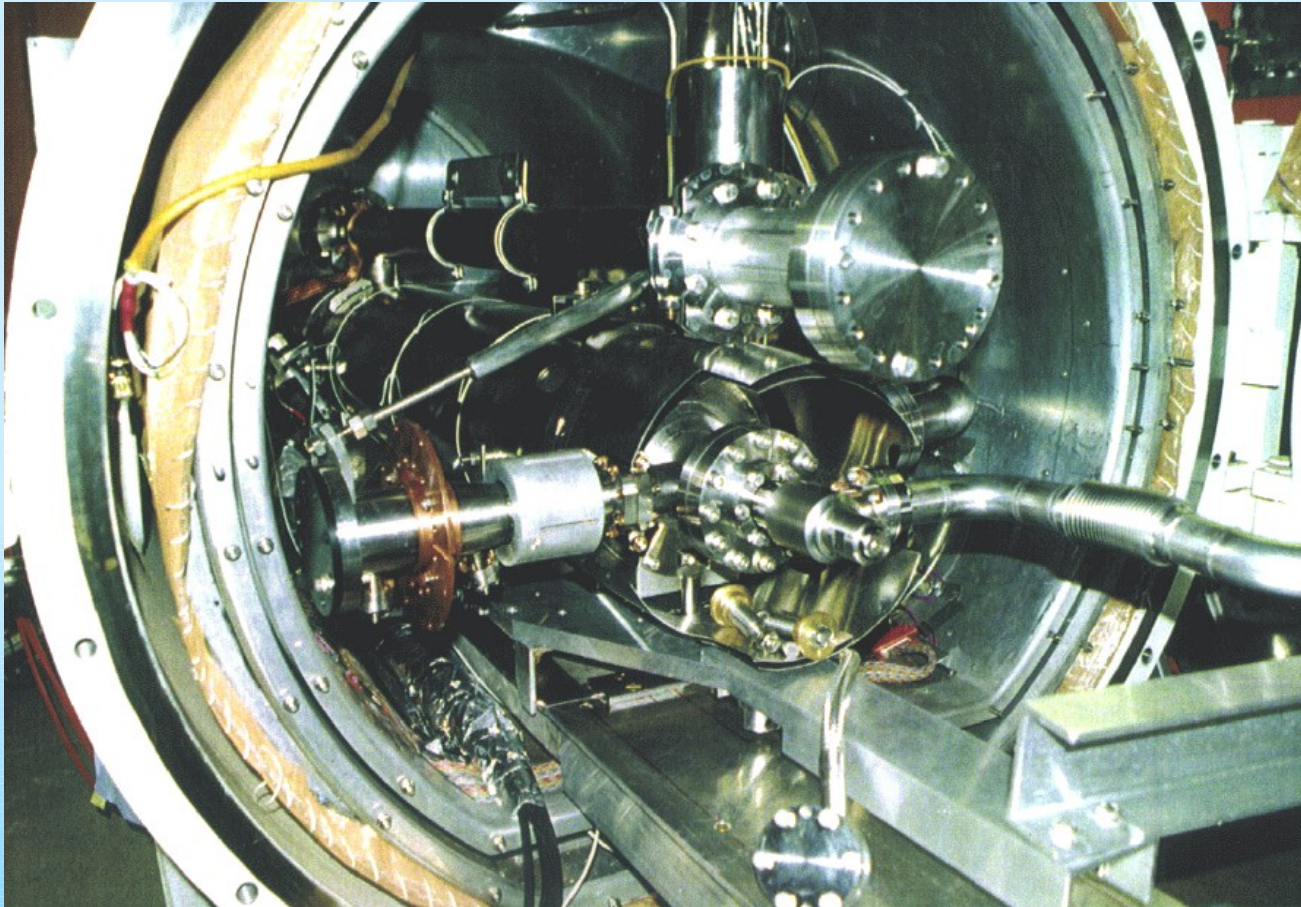
Reference

C. Stolzenburg, "Untersuchungen zur Entstehung von Dunkelströmen in supraleitenden Beschleunigungsstrukturen", (in German); Ph. D. Thesis, University of Hamburg 1996.

CECHIA test facility



seit 1558

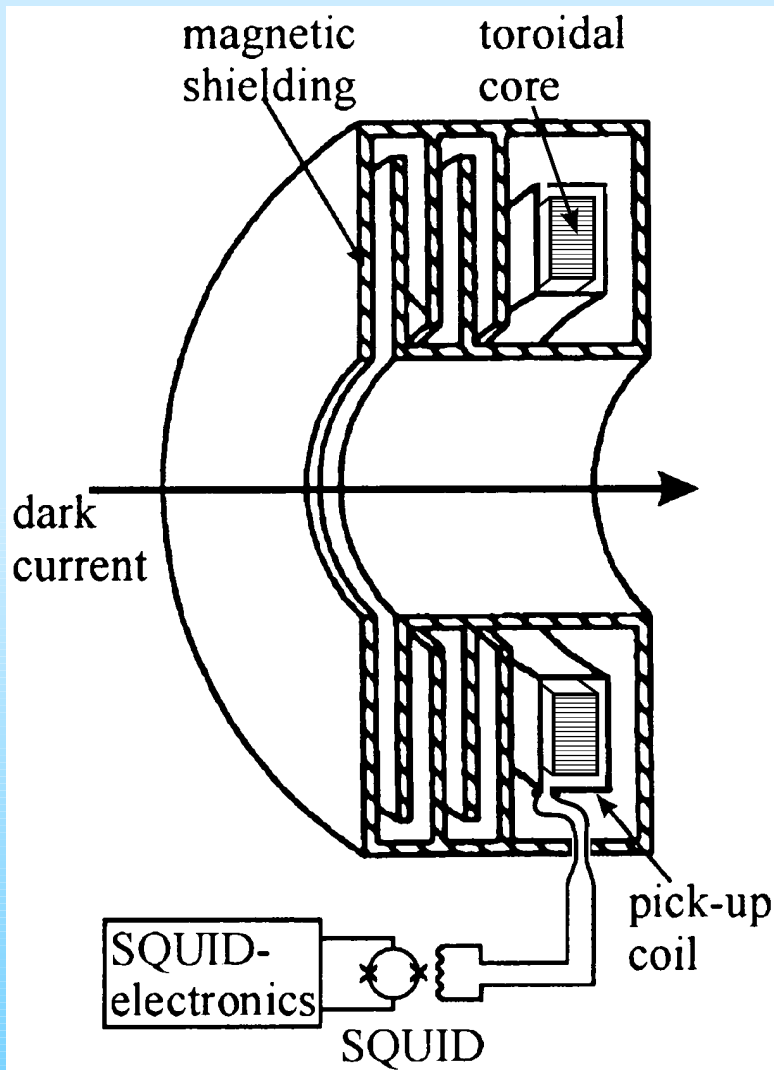


The proof measurements will be performed in the so-called „CHECHIA” test stand at DESY.

Pickup coil with meander-shaped shield



seit 1558

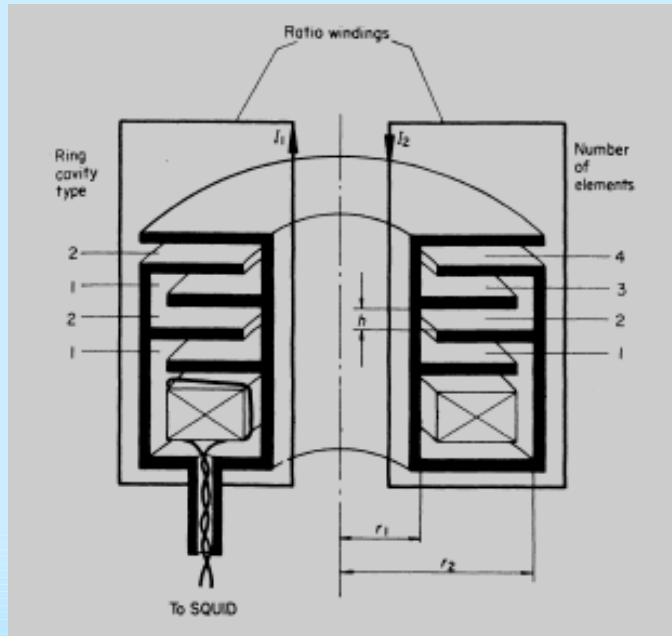


The single turn, superconducting pickup coil is arranged on a toroidal core (VITROVAC, Vakuumschmelze Hanau).

Superconducting shielding



seit 1558



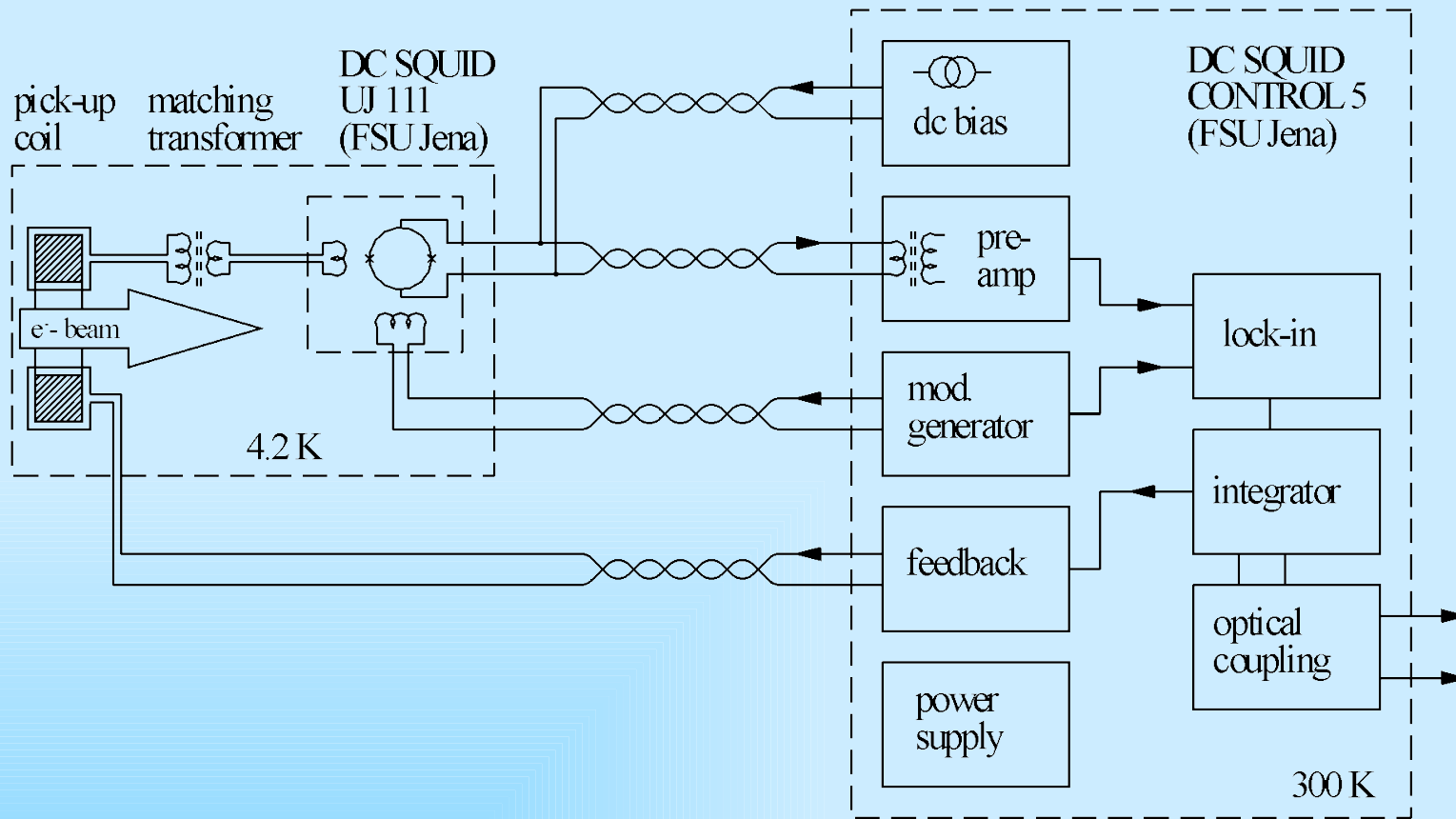
The resolution of the CCC is reduced if the toroidal pickup coil operates in the presence of external magnetic background fields. As this is in practice unavoidable, an effective shielding has to be applied.

- A circular, meander-shaped shielding structure is able to pass the azimuthal magnetic field of the dark current, while strongly attenuating non-azimuthal field components.
- A superconducting shielding material (niobium, lead) leads to an ideal diamagnetic conductor (Meissner-Ochsenfeld effect), providing an expulsion of external magnetic fields.

Electrical scheme of the CCC



seit 1558



A DC-coupled field compensation feedback loop is part of the SQUID electronics. The SQUID input coil and the pickup coil form a superconducting loop, so that the CCC is also able to detect DC-currents.

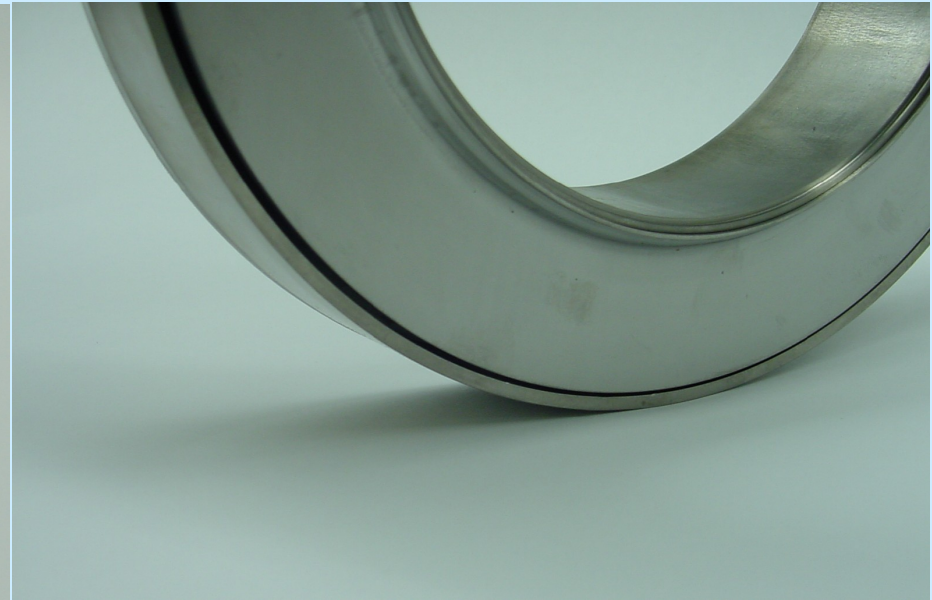
Pick-up coil



seit 1558



Toroidal core (VITROVAC 6025-F)
housed in a VESPEL insulator.

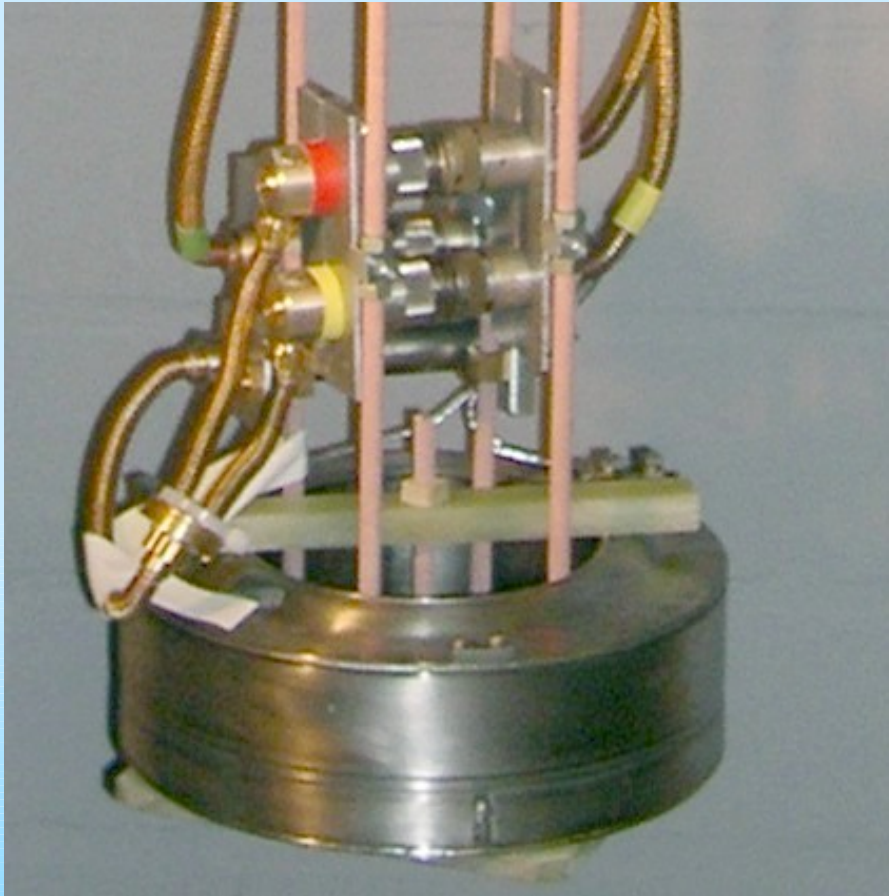


Completed niobium toroidal pick-up coil
with included VITROVAC core.

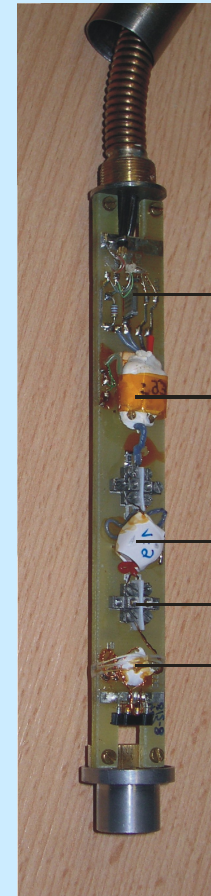
Experimental equipment



seit 1558



The completed niobium pick-up coil of the CCC with all special cabling for the SQUID prepared for low temperature tests in a wide-neck Helium cryostat.

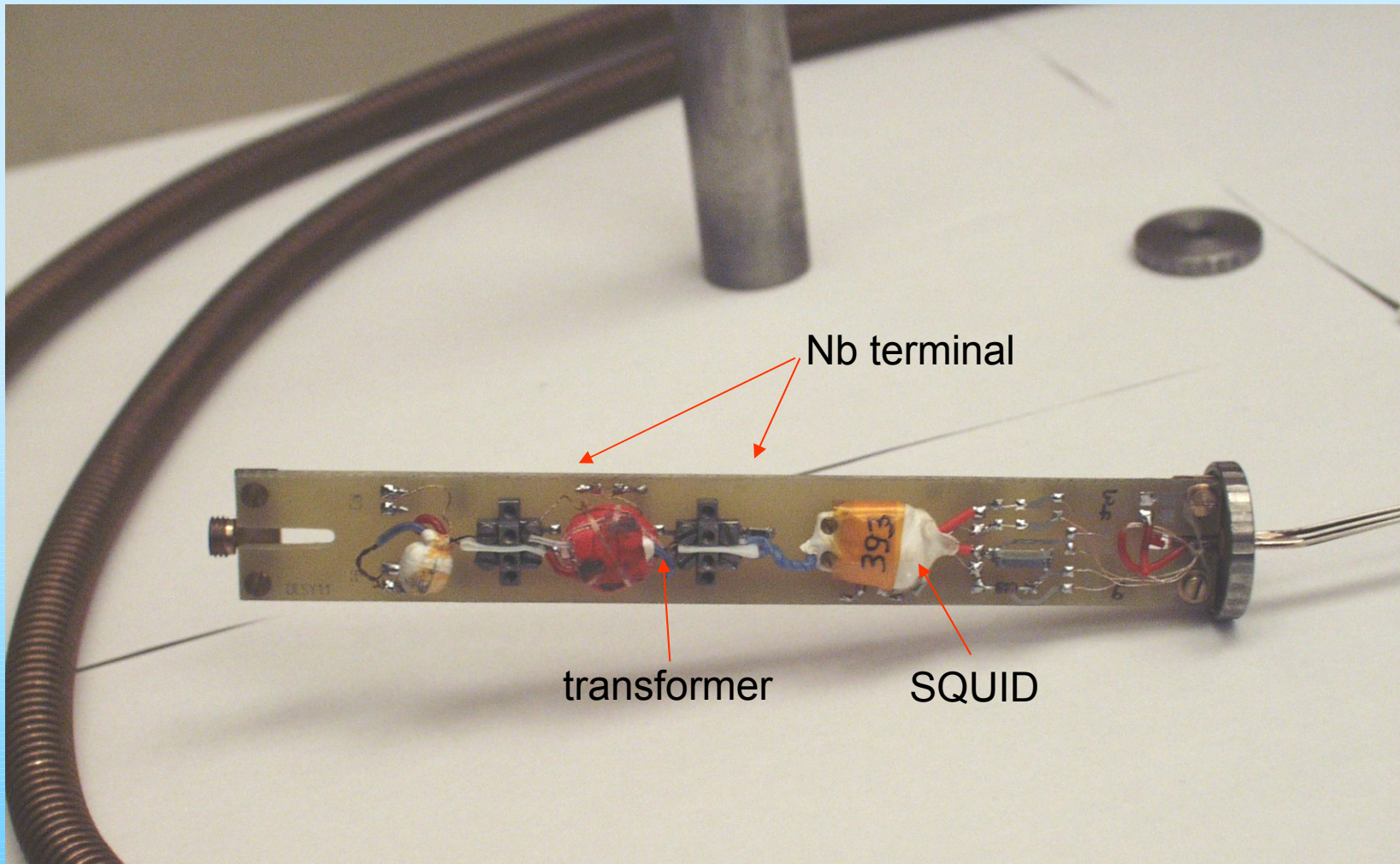


Low temperature probe with LTS SQUID, matching transformer and read-out circuit.

Measuring head with LTS DC-SQUID *UJ 111* (FSU Jena)



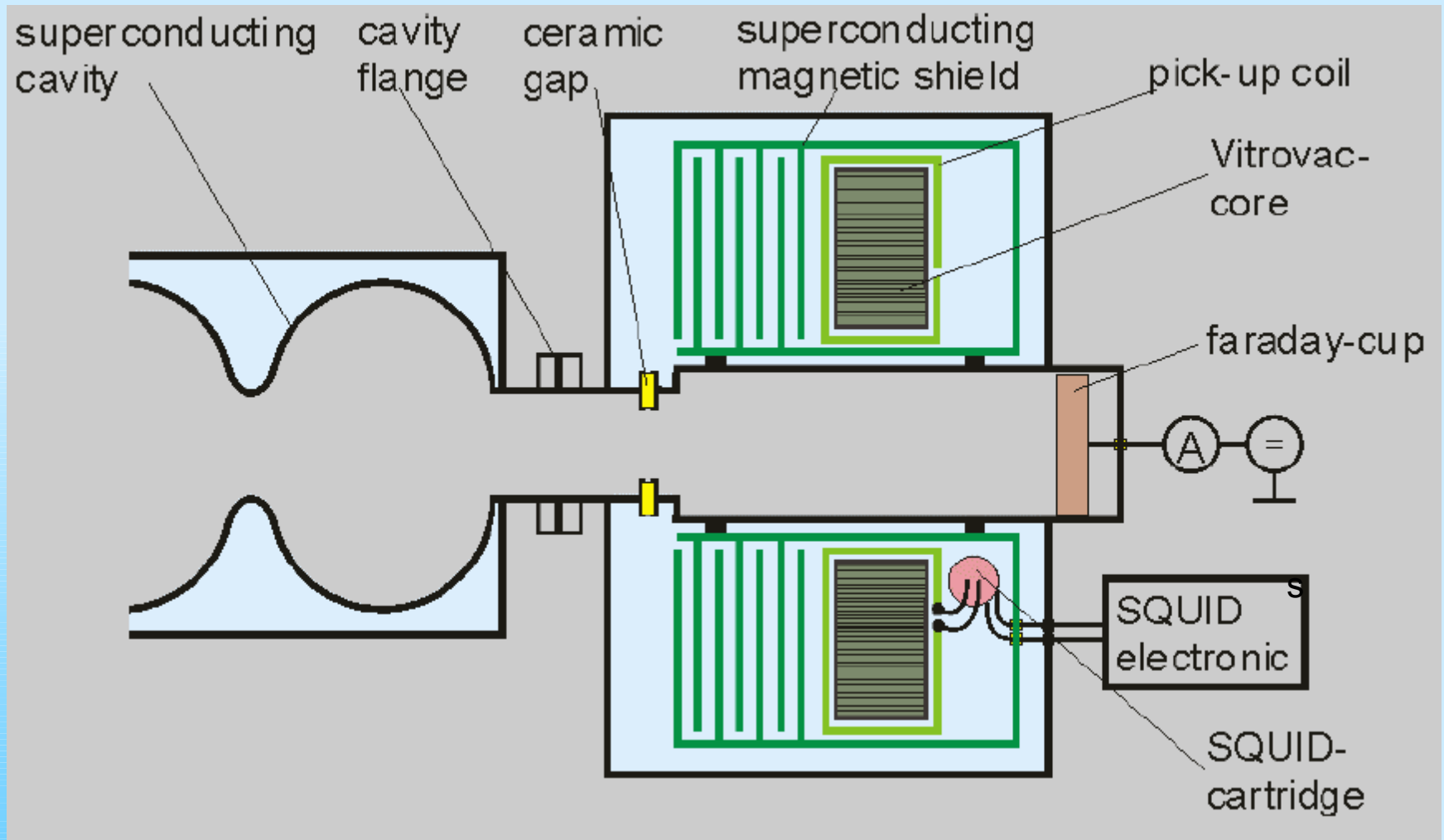
seit 1558



Schematic view of the CCC



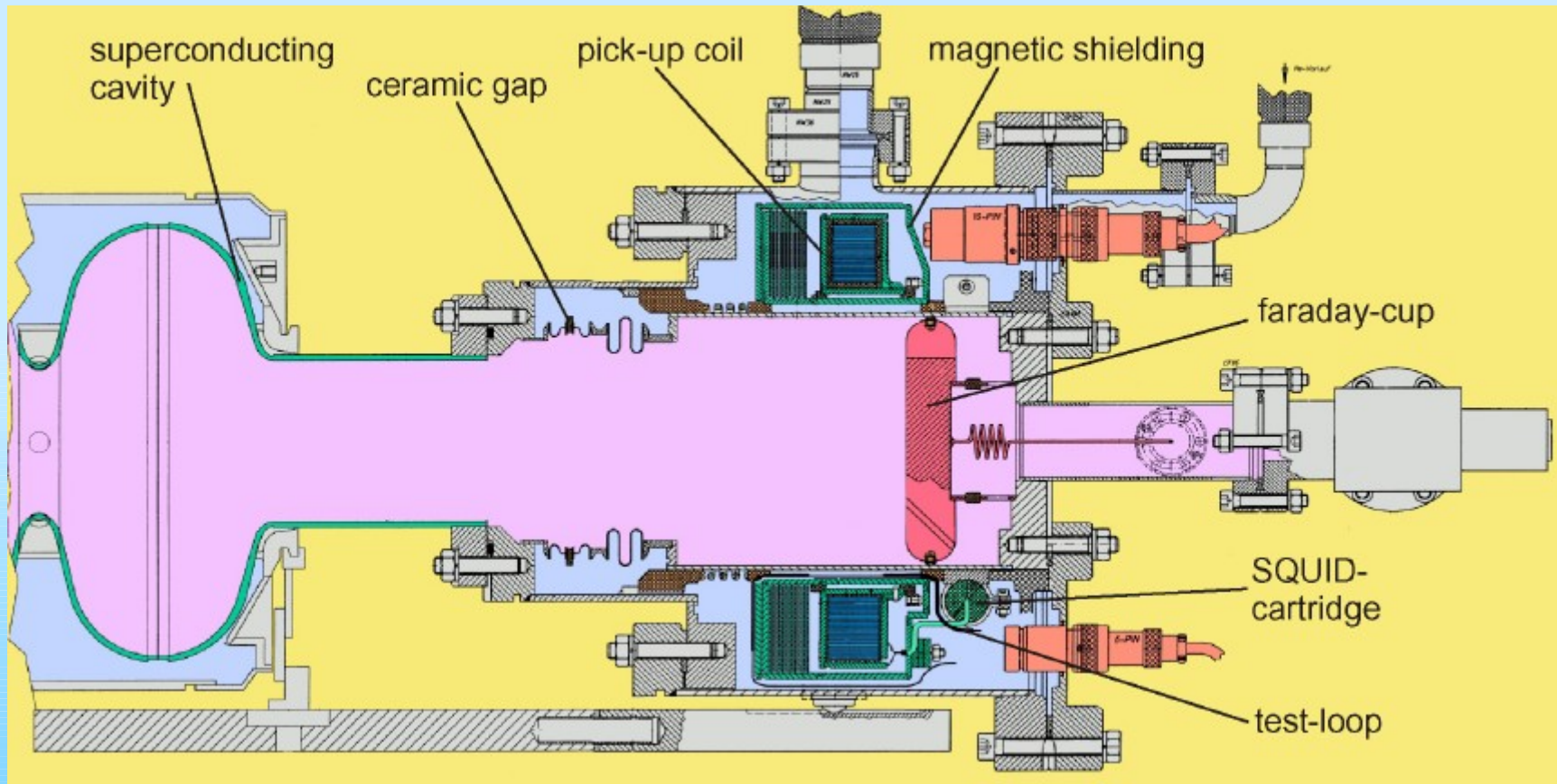
seit 1558



Cross section of the dark current measurement equipment



seit 1558



blue: Liquid Helium
green: Superconductive materials

pink: Ultra high vacuum
yellow: Insulating high vacuum of CHECHIA



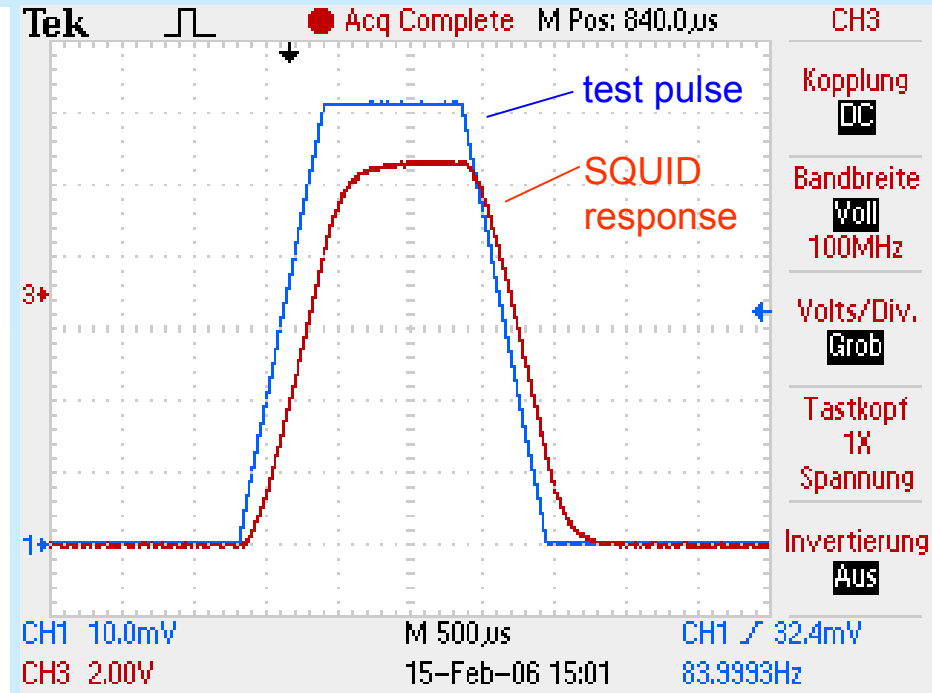
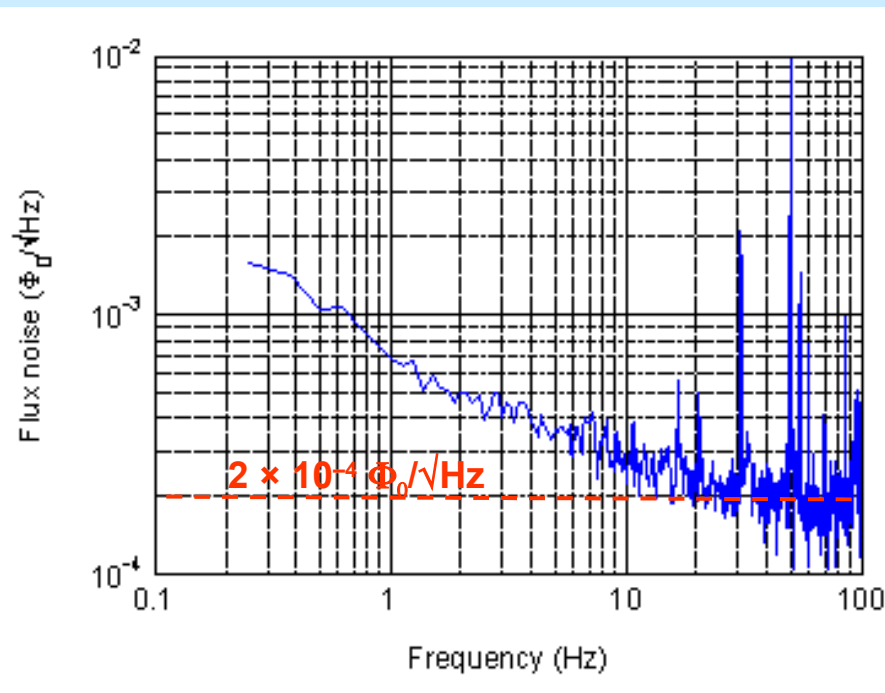
seit 1558

Experimental Results

Noise measurements and SQUID response (with connected pick-up coil)



seit 1558



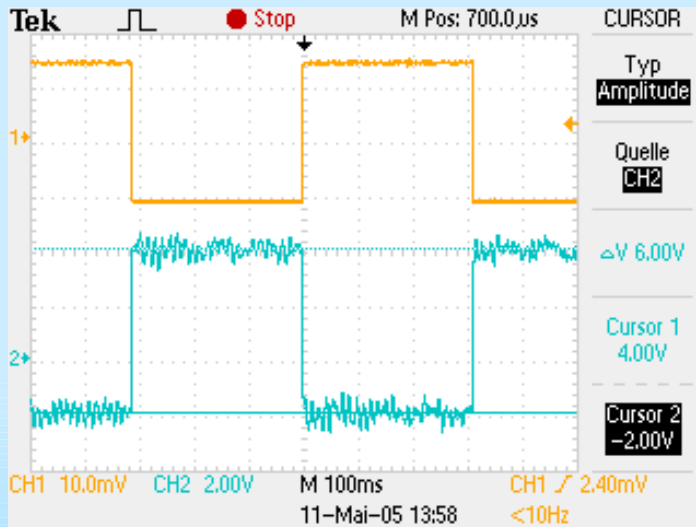
Spectral flux noise density of the SQUID system with connected pick-up coil.

blue: test signal (1 ms current pulse)
red: SQUID system response

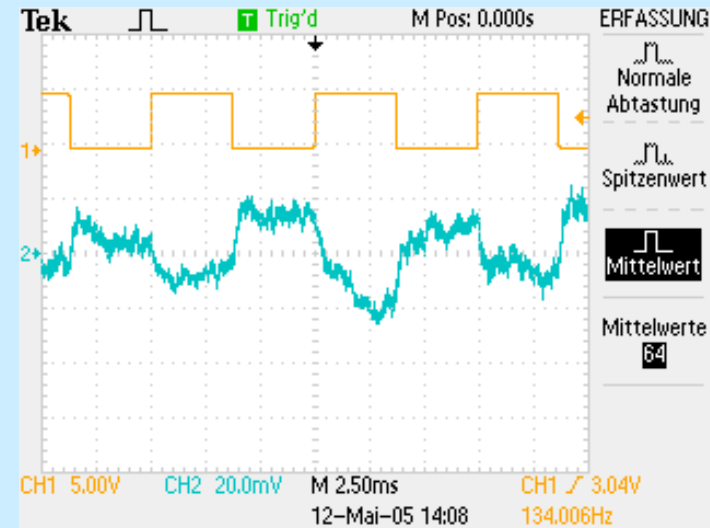
CCC tests with simulated dark current (in the noisy environment at DESY)



seit 1558



126.5 nA current pulse through the calibration coil (upper curve) and SQUID response (lower curve).

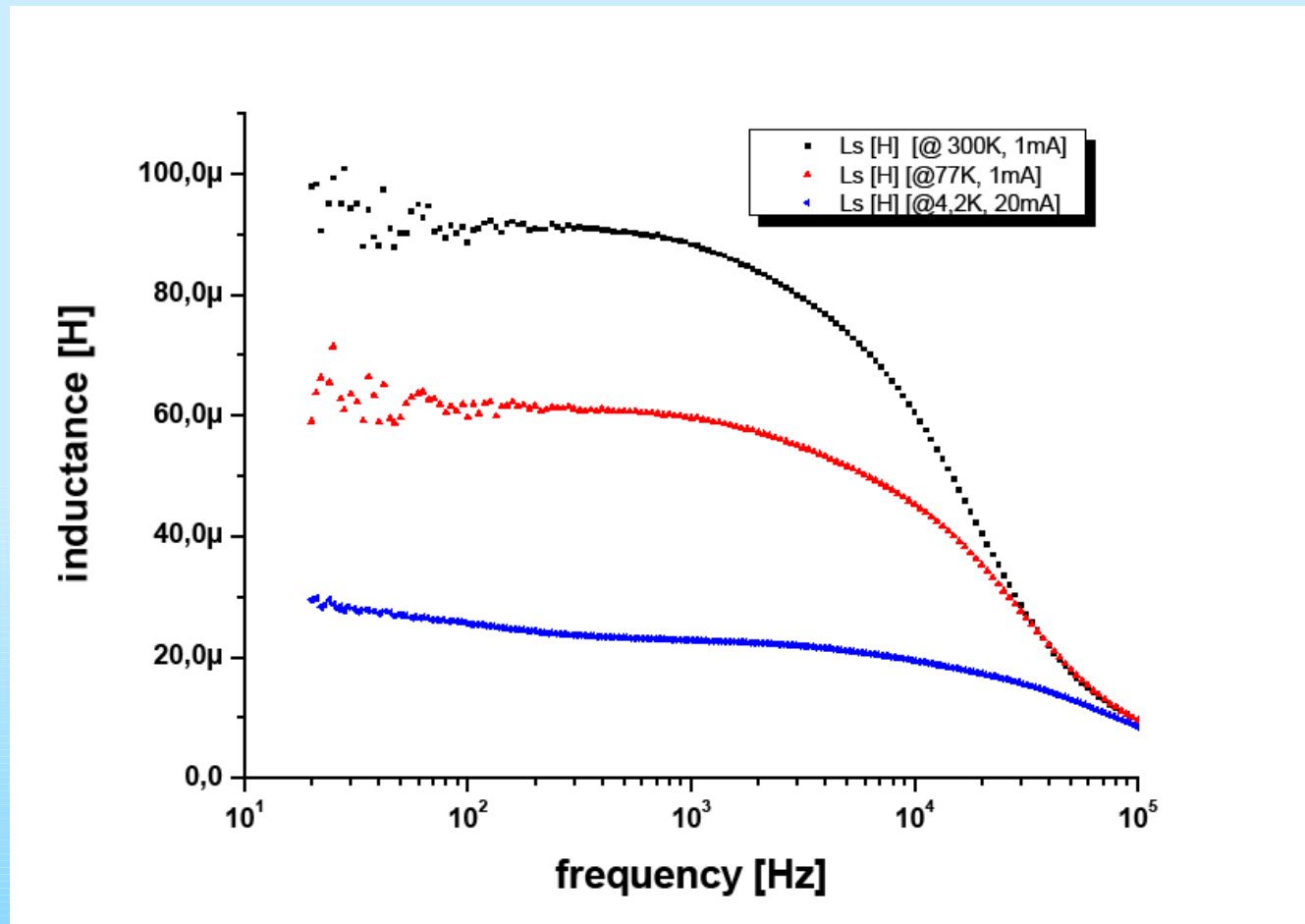


1.3 nA current pulse through the calibration coil (upper curve) and SQUID response (lower curve).

Inductance of pick-up coil



seit 1558

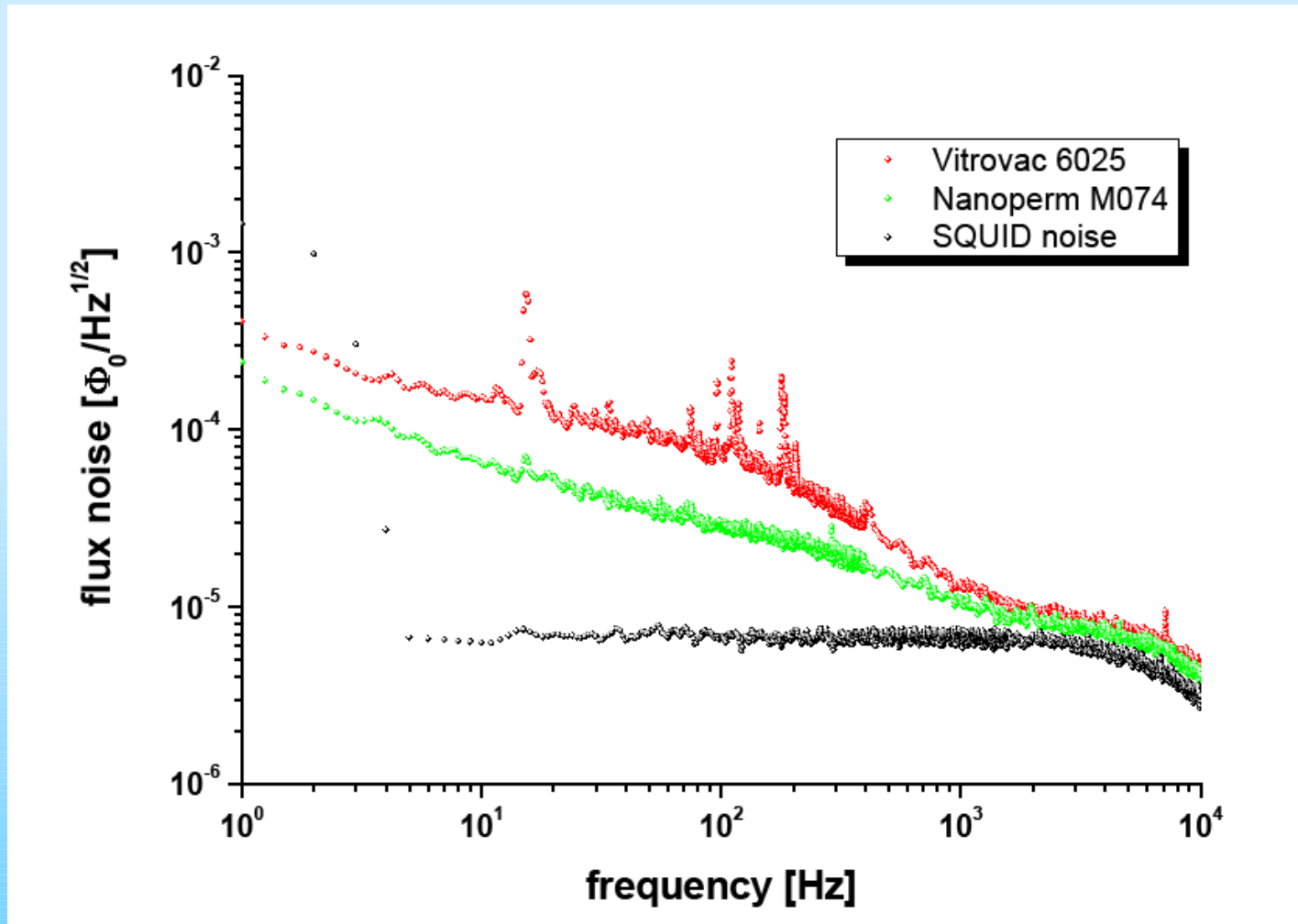


Inductance of the recent pick-up coil of the DESY-CCC in dependence of the frequency at different temperatures.

Spectral flux noise density of the CCC using different core materials



seit 1558





seit 1558

Measured performance of the DESY-CCC

- System bandwidth: dc...70 kHz
- System sensitivity: 167 nA / Φ_0
- Flux noise (in the white noise region): $8 \times 10^{-5} \Phi_0 / \sqrt{\text{Hz}}$
- Corresponding current noise: 13 pA / $\sqrt{\text{Hz}}$

But:

The current resolution of the final system will be decreased due to the additional noise contribution of

- disturbing magnetic background fields and
- mechanical vibrations of environment.

Conclusions and Outlook



seit 1558

- Tests of the pick-up coil with connected SQUID system were successfully done in a wide-neck LHe cryostat.
- The superconducting meander-shaped flux transducer is used to attenuate the magnetic background noise.
- Measurement bandwidth: **dc...70 kHz**
- CCC current sensitivity: **$< 200 \text{ nA}/\Phi_0$**
- Noise limited current resolution (at LT Lab) : **$40 \text{ pA}/\sqrt{\text{Hz}}$**
- Noise limited current resolution (at DESY) : **$500 \text{ pA}/\sqrt{\text{Hz}}$**
- Magnetic flux drift of the CCC: **$< 2 \times 10^{-5} \Phi_0/\text{s}$**

- Currently the DESY-CCC is ready for installation in the HoBiCaT test stand at BESSY.



seit 1558

SQUID-based CCC:

- No back actions
- Highest sensitivity – no alternatives
- Easily calibrated (by electrical current)
- Measurement of absolute current values
- Negligible low drift

Acknowledgment

Co-workers

- R. Neubert
- R. Geithner
- A. Steppke
- S. Hechler

Collaboration

- A. Peters, GSI Darmstadt/HIT Heidelberg
- M. Schwickert, H. Reeg
GSI Darmstadt
- K. Knaack, K. Wittenburg
DESY Hamburg
- T. Siebert, R. von Hahn
MPI Kernphysik, Heidelberg



References

- [1] G. R. Werner, et. al., “Investigation of Voltage Breakdown cause by Microparticles”; Proc. of the Part. Acc. Conf., PAC2001, New York, pp.1071-73
- [2] C. Stolzenburg, “Untersuchungen zur Entstehung von Dunkelströmen in supraleitenden Beschleunigungsstrukturen”, (in German); Ph. D. Thesis, University of Hamburg 1996.
- [3] R. Brinkmann, “Dark Current Issues”; Tesla Collaboration Meeting – CEA SACLAY, 4/2002.
- [4] A. Peters, et. al., “A Cryogenic Current Comparator for the Absolute Measurement of nA Beams”; Proc. of the 8th BIW, Stanford, 1998, AIP Conf. Proc. 451, pp.163-180
- [5] K. Grohmann, et. al.; CRYOGENICS, July 1976, pp.423-429
- [6] K. Grohmann, et. al.; CRYOGENICS, October 1976, pp.601-605
- [7] K. Grohmann and D. Hechtfisher ; CRYOGENICS, October 1977, pp.579-581
- [8] K. Knaack, et. al., “Cryogenic Current Comparator for Absolute Measurements of the Dark Current of Superconducting Cavities of TESLA”; Proc. of the DIPAC 2003, Mainz 2003

Simulated beam signal



seit 1558

